Toll-like receptor 2 and 4 have Opposing Roles in the Pathogenesis of Cigarette Smoke-induced Chronic Obstructive Pulmonary Disease

Tatt Jhong Haw[1,#], Malcolm R. Starkey[1,2,#], Stelios Pavlidis[3], Michael Fricker[1], Anya L. Arthurs[1], Prema M. Nair[1], Gang Liu[1], Irwan Hanish[4], Richard Y. Kim[1], Paul S. Foster[1], Jay C. Horvat[1], Ian M. Adcock[3] and Philip M. Hansbro[1*]

[1]Priority Research Centre for Healthy Lungs, School of Biomedical Sciences and Pharmacy, Hunter Medical Research Institute & University of Newcastle, Callaghan, New South Wales, Australia

[2]Priority Research Centre for Grow Up Well, School of Biomedical Sciences and Pharmacy, Hunter Medical Research Institute & University of Newcastle, University of Newcastle, Callaghan, New South Wales, Australia

[3]The Airways Disease Section, National Heart & Lung Institute, Imperial College London, London, UK

[4]Department of Microbiology, Faculty of Biotechnology and Biomolecular Sciences, Universiti Putra Malaysia, Serdang, Selangor, Malaysia

Running header: Opposing roles of TLR2 and TLR4 in pathogenesis of COPD

Author contributions: TJH, MRS and PMH designed the study. TJH and MRS performed the experiments, collected and analyzed the data, generated the figures, and wrote the manuscript. SP analyzed and generated the human data. MF and ALA analyzed and generated isolated lung macrophage data. PMN, GL, IH and RYK assisted in performing the experiments and collecting the data. JCH advised on experimental design and analysis and edited the manuscript. IMA analyzed the human data and edited the manuscript. PMH oversaw the project and advised on collection and analysis of data and edited the manuscript.

[#] TJH and MRS contributed equally to this work

*Corresponding author: Philip M. Hansbro, PhD, Priority Research Centre for Healthy Lungs, School of Biomedical Sciences and Pharmacy, Hunter Medical Research Institute & University of Newcastle, Callaghan, New South Wales 2308, AUSTRALIA. Telephone: (+61) 40420187 Email: Philip.Hansbro@newcastle.edu.au

ABSTRACT

Chronic Obstructive Pulmonary Disease (COPD) is the third leading cause of morbidity and death and imposes major socioeconomic burdens globally. It is a progressive and disabling condition that severely impairs breathing and lung function. There is a lack of effective treatments for COPD, which is a direct consequence of the poor understanding of the underlying mechanisms involved in driving the pathogenesis of the disease. Toll-like receptor (TLR)2 and TLR4 are implicated in chronic respiratory diseases, including COPD, asthma and pulmonary fibrosis. However, their roles in the pathogenesis of COPD are controversial and conflicting evidence exists. In the current study, we investigated the role of TLR2 and TLR4 using a model of cigarette smoke (CS)-induced experimental COPD that recapitulates the hallmark features of human disease. TLR2, TLR4 and associated co-receptor mRNA expression were increased in the airways in both experimental and human COPD. Compared to WT mice, CS-induced pulmonary inflammation was unaltered in TLR2-deficient (*Tlr2*$^{-/-}$), TLR4-deficient (*Tlr4*$^{-/-}$) mice. CS-induced airway fibrosis, characterized by increased collagen deposition around small airways, was not altered in *Tlr2*$^{-/-}$ mice but was attenuated in *Tlr4*$^{-/-}$ mice compared to CS-exposed WT controls. However, *Tlr2*$^{-/-}$ mice had increased CS-induced emphysema-like alveolar enlargement, apoptosis and impaired lung function, whilst these features were reduced in *Tlr4*$^{-/-}$ mice compared to CS-exposed WT controls. Taken together, these data highlight the complex roles of TLRs in the pathogenesis of COPD and suggest that activation of TLR2 and/or inhibition of TLR4 may be novel therapeutic strategies for the treatment of COPD.

Key words: TLR2, TLR4, cigarette smoke, emphysema, COPD

INTRODUCTION

Chronic Obstructive Pulmonary Disease (COPD) is the third leading cause of morbidity and death and imposes significant socioeconomic burden worldwide (63). It is a complex, heterogeneous disease characterized by chronic pulmonary inflammation, emphysema and airway remodeling, which are associated with progressive lung function decline (39). Indeed, the major disease features are progressive and become more severe over time that is accelerated by infection-induced exacerbations. Cigarette smoke (CS) is a major risk factor for COPD (54). The current mainstay therapies for COPD are glucocorticoids, β_2-adrenergic receptor agonists and long acting muscarinic antagonists (5, 93). However, these agents are largely ineffective and only provide symptomatic relief rather than modifying the causal factors or stopping disease progression (5). There is much current interest in increased microbial carriage and altered lung and gut microbiomes in COPD that could be modified for therapeutic gain and macrolide antibiotics are currently being tested as new treatments (14, 89, 92). Nevertheless, there is currently a lack of effective treatments for COPD that is largely due to the poor understanding of the underlying mechanisms.

Toll-like receptor (TLR)2 and TLR4 play vital roles in detecting and initiating immune responses to microbial membrane components (1, 36, 52). TLR2 and TLR4 are type I transmembrane receptors expressed on the cell surface (1, 36, 52). However, in some circumstances TLR4 can be internalized or expressed intracellularly in certain cells (1, 36, 52). TLR2 and TLR4 primarily signal through the adaptor protein myeloid differentiation primary response gene 88 (MyD88)-dependent or MyD88-adapter-like (Mal)-dependent pathways (1, 36, 52). Upon ligand (e.g. bacterial peptidoglycan) binding, TLR2 forms a heterodimer with either TLR1 or TLR6 and interacts with cluster of differentiation (CD)14 to form a functional complex (24, 48). In contrast, TLR4 forms a homodimer upon binding to its

ligand (e.g. bacterial lipopolysaccharide) and interacts with CD14 and/or MD2 (also known as lymphocyte antigen 96 [LY96] in humans) (57, 108). This initiates the recruitment of MyD88 to the intracellular Toll–interleukin 1 (IL-1) receptor (TIR) domain, that subsequently activates members of the IL-1 receptor-associated kinases (IRAKs) and tumor necrosis factor (TNF) receptor-associated factor 6 (TRAF6) (1, 52). Consequently, transcriptional factors of the mitogen-activated protein kinase (MAPK) family and nuclear factor kappa-light-chain-enhancer of activated B cells (NF-κB) are activated, leading to the expression of pro-inflammatory mediators (1, 36, 52).

TLR2 and TLR4 are widely implicated in chronic respiratory diseases, including asthma and pulmonary fibrosis (18, 25, 37, 42, 55, 56, 58, 59, 82, 86, 90, 106). Both are associated with increased susceptibility to asthma and allergies in children (25, 55). In adults, increased expression of TLR2, TLR4 and CD14 were observed in subjects with bronchiectasis and asthma (90). These observations were supported by findings from mouse models of allergic airway disease (18, 37, 59, 82, 106) and bleomycin-induced pulmonary fibrosis (42, 56, 58, 60, 86). We have also shown that TLR2 was essential in protecting against early-life respiratory infection and the development of subsequent chronic lung disease in later life (6, 27, 44, 96, 97). However, the role of TLR2 and TLR4 in the pathogenesis of COPD remains controversial and conflicting evidence exists in the literature. Some studies show that TLR2 and TLR4 expression are increased by CS exposure or in COPD patients (3, 21, 30, 33, 66, 69, 75, 80, 85, 91). However, others show that these TLRs are either not altered or are decreased by CS exposure or in COPD patients (22, 65, 80, 87).

Hence, the role of TLR2 and TLR4 in the pathogenesis of COPD remains unclear. Here, we investigated these roles using an established mouse model of CS-induced experimental COPD that recapitulates the critical features of human disease (7, 29, 31, 40, 41, 47, 62, 100) as well as gene expression analysis of lung tissues from human COPD

patients. TLR2, TLR4 and associated co-receptor mRNA were increased in the airways in both experimental and human COPD. Compared to WT controls, CS-induced pulmonary inflammation was largely unaltered in TLR2-deficient (*Tlr2*$^{-/-}$) and TLR4-deficient (*Tlr4*$^{-/-}$) mice. However, *Tlr2*$^{-/-}$ mice had increased CS-induced emphysema-like alveolar enlargement, apoptosis and impaired lung function whilst CS-induced airway fibrosis was not altered. In contrast, these features were reduced or completely attenuated in *Tlr4*$^{-/-}$ mice compared to WT controls, thus implicating this TLR in the pathogenesis of COPD.

MATERIALS AND METHODS

Ethics statement. This study was performed in accordance with the recommendations issued by the National Health and Medical Research Council of Australia. All experimental protocols were approved by the animal ethics committee of The University of Newcastle, Australia.

Experimental COPD. Female, 7-8-week-old, wild-type (WT), *Tlr2*$^{-/-}$ or *Tlr4*$^{-/-}$ BALB/c mice were purchased from the Australian Bioresource Facility, Moss Vale, NSW, Australia. *Tlr2*$^{-/-}$ and *Tlr4*$^{-/-}$ mice were generous gifts from Prof. Shizuo Akira, Osaka University, Japan and generated by using targeting vectors that introduce a targeted mutation in the mouse *Tlr2* and *Tlr4* genes as previously described (46, 99). Mice were housed under a 12-hour light/dark cycle and had free access to food (standard chow) and water. After period of acclimatization (up to 5 days), mice were randomly placed into experimental groups and exposed to either normal air or nose-only inhalation of CS for up to twelve weeks as described previously (7, 29, 31, 40, 41, 47, 62, 100). Recently, studies have shown that COPD prevalence and

mortality are higher in females, and in the United States in 2009 women accounted for 53% of COPD deaths (78). It is for these and logistical reasons that female mice are used.

Isolation of RNA and qPCR. Total RNA was extracted and reversed transcribed from whole lung tissue, blunt-dissected airway and parenchyma and isolated lung macrophages (7, 41, 70, 101). mRNA transcripts were determined by real-time quantitative PCR (qPCR, ABIPrism7000, Applied Biosystems, Scoresby, Victoria, Australia) using custom designed primers (Integrated DNA Technologies, Baulkham Hills, New South Wales, Australia), normalized to the reference gene hypoxanthine-guanine phosphoribosyltransferase (HPRT) and expressed as relative abundance to WT air controls (**Table 1**) (7, 41, 70, 101).

Immunohistochemistry. Lungs were perfused, inflated, formalin-fixed, paraffin-embedded and sectioned (4-6μm). Longitudinal sections of the left lung were rehydrated through a series of xylene (2x) and ethanol gradient (2x absolute, 90%, 80%, 70%, 50%, 0.85% saline and phosphate-buffered saline [PBS]) washes followed by antigen retrieval with citrate buffer (10mM citric acid, 0.05% Tween 20, pH 6.0) at 100°C for 30 mins. Sections were blocked with casein blocker (Thermo Fisher Scientific, Pittsburgh, PA, USA) for 1 hour. Sections were then washed with PBS (5x, 5 mins each) and incubated with either anti-TLR2 (1:200 dilution, MABF84, clone 19B6.2, Merck Milipore, Bayswater, Victoria, Australia), anti-TLR4 (1:1000 dilution, ab47093, Abcam, Melbourne, Victoria, Australia) or anti-active caspase-3 (1:200 dilution, ab13847, Abcam) antibodies followed by either anti-rabbit (HAF008; R&D Systems, Gymea, New South Wales, Australia) or anti-mouse (ab6728; Abcam) secondary antibody conjugated with horseradish peroxidase and then 3,3'-Diaminobenzidine chromogen-substrate buffer (DAKO, North Sydney, New South Wales,

Australia) according to manufacturer's instructions (40, 41). Sections were counterstained with hematoxylin, mounted and analyzed using a BX51 microscope (Olympus, Tokyo, Shinjuku, Japan) with Image-Pro Plus software (Media Cybernetics, Rockville, MD). The areas of active caspase-3 in lung parenchyma were determined (n=4 per group, 10 randomized parenchyma images per lung sections) using ImageJ software (Version 1.50, NIH, New York City, NY, USA), normalized to area of hematoxylin and represented as the percentage area of active caspase-3. Images with inflammation and airways were excluded from analysis.

Isolation of lung macrophages. Lungs were excised, washed and dissected into 1-2mm cubes in Dulbecco's Modified Eagle Medium (DMEM, Sigma Aldrich, Castle Hill, New South Wales, Australia). Lung tissues were then transferred into Medicon cassettes (BD Biosciences, North Ryde, New South Wales, Australia) and disaggregated using a Medimachine (BD Biosciences) for 2 mins. Cell suspensions were collected, Histopaque 1083 (Sigma Aldrich) applied and centrifuged (825x*g*, 30 mins, 22.5 °C). The opaque interface cell layer where macrophages/monocytes were enriched was collected, washed with Hyclone™ Dulbecco's PBS (GE Healthcare Life Sciences, South Logan, Utah, USA) and centrifuged (100x*g*, 5 mins, 22.5 °C). Cell pellets were resuspended in fresh DMEM (Sigma) and macrophages further enriched through adherence to plastic tissue culture flasks (3 hrs, 37 °C). Non-adherent contaminating cells were removed by gentle washing with PBS (GE Healthcare Life Sciences) prior to RNA isolation.

Flow Cytometry Analysis. The numbers of $CD11b^{+}$ monocytes, neutrophils and myeloid dendritic cells (mDCs) in lung homogenates were determined based on surface marker

expression using flow cytometry (**Table 2**) (45, 53, 94, 97, 101). Flow cytometric analysis was performed using a FACSAriaIII with FACSDiva software (BD Biosciences, North Ryde, Australia). Flow cytometry antibodies were purchased from Biolegend (Karrinyup, Western Australia, Australia) or BD Biosciences (**Table 3**). OneComp compensation beads (Thermo Fisher Scientific) were used to compensate for spectral overlap.

Gene Expression in Human COPD Microarray Datasets. Analysis of TLR2, TLR4 and co-receptors gene expression in published human array datasets (Affymetrix Human Genome U133 Plus 2.0 Array, Accession numbers: GSE5058 and GSE27597) (13, 16, 102) were performed using the Array Studio software (Omicsoft Corporation, Research Triangle Park, NC, USA) by applying a general linear model adjusting for age and gender and the Benjamini–Hochberg method for p-value adjustment (41). Data are expressed as $\log_2$ intensity robust multi-array average signals. The Benjamini–Hochberg method for adjusted P value/false discovery rate (FDR) was used to analyze differences between two groups. Statistical significance was set at FDR < 0.05.

Pulmonary Inflammation. Airway inflammation was assessed by differential enumeration of inflammatory cells in bronchoalveolar lavage fluid (BALF) (7, 27, 40, 41, 62, 70). Lung sections were stained with periodic acid-Schiff (PAS) and tissue inflammation assessed by enumeration of inflammatory cells (7, 41, 70). Histopathological score was determined in lung sections stained with hematoxylin and eosin (H&E) based on established custom-designed criteria (40, 44, 70).

Enzyme-linked immunosorbent assay (ELISA). Right lung lobes were homogenized on ice in 500uL of PBS supplemented with Complete mini protease inhibitor cocktail (Roche Diagnostic, Sydney, NSW, Australia) and PhosphoSTOP tablets (Roche Diagnostic). Lung homogenates were incubated on ice for 5 mins and subsequently centrifuged (8,000x*g*, 15 mins). Supernatants were collected, stored at -20°C overnight and total protein levels were determined using Pierce BCA assay kit (Thermo Fisher Scientific) prior to ELISA. TNFα protein levels were quantified with mouse TNFα Duoset ELISA kit as per manufacturer's instructions (R&D systems). TNFα protein levels were normalized to total protein in lung homogenates. Hyaluronan protein levels in BALF were quantified with mouse hyaluronan Quantikine ELISA kits as per manufacturer's instructions (R&D systems).

Airway Remodeling. Lung sections were stained with PAS or Masson's Trichrome. Airway epithelial area (μm^2), cell (nuclei) number and collagen deposition area (μm^2) were assessed in a minimum of four small airways (basement membrane [BM] perimeter <1,000μm) per section (7, 40, 41, 62, 70). Data were quantified using ImageJ software (Version 1.50, NIH) and normalized to BM perimeter (μm).

Alveolar Enlargement. Lung sections were stained with H&E. Alveolar septal damage and diameter were assessed by using the destructive index technique (26) and mean linear intercept technique respectively (7, 41, 47, 62).

Apoptosis. Lung sections were stained with terminal deoxynucleotidyl transferase dUTP nick end labeling (TUNEL) assay kits (Promega, Sydney, New South Wales, Australia) according

to manufacturer's instructions (41). Apoptosis in lung parenchyma was assessed by enumerating the numbers of $TUNEL^+$ cells per high power fields (HPF; 100x) (41).

Lung Function. Mice were anaesthetized with ketamine (100mg/kg) and xylazine (10mg/kg, Troy Laboratories, Smithfield, Australia) prior to tracheostomy. Tracheas were then cannulated and attached to Buxco® Forced Maneuvers systems apparatus (DSI, St. Paul, Minnesota, USA) to assess total lung capacity (TLC) (7, 40). Mice were then attached to a FlexiVent apparatus (FX1 System; SCIREQ, Montreal, Canada) to assess transpulmonary resistance (tidal volume of 8mL/kg at a respiratory rate of 450 breaths/mins) (7). All assessments were performed at least three times and the average was calculated for each mouse.

Statistical analyses. Data are presented as means ± standard error of mean (SEM) and representative from two independent experiments with 6 mice per group. The two-tailed Mann-Whitney test was used to compare two groups. The one-way analysis of variance with Bonferroni post-test was used to compare 3 or more groups. Statistical significance was set at $P < 0.05$ and determined using GraphPad Prism Software version 6 (San Diego, CA, USA).

RESULTS

TLR2 and TLR4 mRNA Expression and Protein Levels are Increased in CS-induced Experimental COPD

To determine whether TLR2 and TLR4 levels are altered in COPD, we first interrogated our mouse model of experimental COPD (7, 29, 31, 40, 41, 47, 62, 100). WT mice were exposed to CS for 4, 8 and 12 weeks and TLR2 and TLR4 mRNA expression were assessed. TLR2, but not TLR4 mRNA was significantly increased in whole lung homogenates after 4, 8 and 12 weeks of CS exposure compared to normal air-exposed mice (Figure 1A-B). We have previously shown that many of the hallmark features of COPD were established in mice after 8 weeks of CS exposure (7, 29, 31, 40, 41, 47, 62, 100). To determine the compartment of the lung in which altered TLR2 and TLR4 expression occurred following establishment of disease, blunt dissected airways and lung parenchyma were assessed at this time point. To confirm separation of blunt dissected airways from parenchymal tissue we assessed the mRNA expression of airway epithelial cell-specific mucin 5ac (Muc5ac) and the mouse type II alveolar epithelial cell-marker surfactant protein C (Sftpc) in normal air-exposed mice (Figure 1C). The levels of Muc5ac mRNA were increased in airways compared to lung parenchyma. Conversely, the levels of Sftpc mRNA were increased in lung parenchyma compared to airways. This confirms the tissue specific isolation and location of TLR2, TLR4 and co-receptors in these tissues. TLR2 mRNA was increased in both the airways and parenchyma of CS-exposed mice (Figure 1D-E). In contrast, TLR4 mRNA was increased in the airways, but not parenchyma (Figure 1F-G). These mRNA expression data were supported by increased TLR2 (Figure 1H-I) and TLR4 (Figure 1J-K) protein levels in small airway epithelial cells and increased infiltration of parenchyma-associated inflammatory cells that expressed TLR2 or TLR4 in lung histology sections detected by immunohistochemistry.

To identify the inflammatory cell source of TLR2 and TLR4, macrophages were isolated from whole lung homogenates for downstream mRNA analysis. Interestingly, the mRNA expression of TLR2 and TLR4 were not altered in lung macrophages isolated from CS-exposed mice (Figure 2A-B). $CD11b^{+}$ monocytes, neutrophils and mDCs are known to

express TLR2 and/or TLR4 (6, 10, 80, 81), and have roles in COPD pathogenesis (41, 91). Thus, we next determined whether CS altered the numbers of these immune cells that expressed TLR2 and/or TLR4 in the lung using flow cytometry. CS-exposed mice had increased the numbers of $CD11b^+$ monocytes that expressed TLR2 ($TLR2^+$), but not those that expressed TLR4 ($TLR4^+$) or co-expressed TLR2 and TLR4 ($TLR2^+TLR4^+$) (Figure 2C) compared to normal air-exposed controls. In contrast, CS-exposed mice had significantly increased numbers of neutrophils and mDCs that were either $TLR2^+$, $TLR4^+$ or $TLR2^+TLR4^+$ (Figure 2D-E) compared to normal air-exposed controls.

TLR2 and TLR4 Co-receptor mRNA Expression are Increased in CS-induced Experimental COPD

When activated, TLR2 and TLR4 interact with co-receptors TLR1, TLR6, CD14 and/or MD2/Ly96 to mediate inflammatory responses (1, 36, 52). Therefore, we next determined whether the mRNA expression of these co-receptors was altered by CS exposure. TLR1 mRNA was increased in blunt dissected lung parenchyma, but not airways compared to normal air-exposed controls (Figure 3A-B). In contrast, TLR6 and CD14 mRNA were increased in both airways and parenchyma (Figure 3C-F). MD2/Ly96 mRNA expression was not altered by CS exposure (Figure 3G-H).

TLR2, TLR4 and Co-receptor mRNA Expression are Increased in the Airways in Human COPD

We next sought to determine whether the mRNA expression of TLR2, TLR4 and their co-receptors were altered in humans with mild-to-moderate COPD (Global Initiative for Chronic

Obstructive Lung Disease [GOLD] Stage I or II (103)). Pre-existing microarray data from non-COPD (healthy non-smokers and healthy smokers) and COPD patients were interrogated (13, 16, 102). TLR2, TLR4 and co-receptor (TLR1, TLR6, CD14 and LY96) mRNA expression were not significantly altered in airway epithelial brushings from healthy smokers compared to non-smokers (Accession: GSE5058 (102), Figure 4A-F). Importantly, however, TLR2 (~2.4-fold), TLR4 (~8.7-fold), TLR1 (~7.1-fold), TLR6 (~1.5-fold), CD14 (~3.9-fold) and LY96 (~12.9-fold) mRNA expression were increased in airway epithelial brushings from patients with mild-to-moderate COPD compared to non-smokers. Notably, TLR2 (~2.4-fold), TLR4 (~7.2-fold), TLR1 (~4.7-fold), CD14 (~3.6-fold) and LY96 (~6.8-fold) but not TLR6 (~0.8-fold) mRNA expression were also increased in airway brushings from COPD patients compared to healthy smokers (Figure 4A-F).

TLR2, TLR4 and Co-receptor mRNA Expression are Decreased in the Parenchyma in Human COPD

Similarly, we then assess the expression of TLR2, TLR4 and co-receptor expression in pre-existing microarray data from lung parenchyma cores from severe COPD patients (GOLD Stage IV (103)) compared to non-smokers without COPD (Accession: GSE27597 (13, 16)). In contrast to the data from the airways, TLR2 (~1.5-fold) and TLR4 (~2.0-fold) expression were reduced, whereas co-receptors TLR1, TLR6 and LY96 were not altered, in the parenchyma from severe COPD patients compared to non-smokers without COPD (Figure 4G-K). CD14 was not detectable in this dataset.

CS-induced Pulmonary Inflammation was Largely Unaltered in TLR2-deficeint and TLR4-deficient mice with Experimental COPD

We next investigated whether TLR2 and TLR4 play a role in the pathophysiology of CS-induced experimental COPD. WT, *Tlr2*$^{-/-}$ and *Tlr4*$^{-/-}$ mice were exposed to normal air or CS for 8 weeks (7, 29, 31, 40, 41, 47, 62, 100). We first assessed pulmonary inflammation in BALF by staining and differential enumeration of inflammatory cells. As expected, CS-exposure of WT mice resulted in significantly increased total leukocytes, macrophages, neutrophils and lymphocytes in BALF compared to normal air-exposed WT controls (Figure 5A-D). CS-exposed *Tlr2*$^{-/-}$ mice had increased neutrophils and lymphocytes, but not total leukocytes and macrophages, compared to normal air-exposed *Tlr2*$^{-/-}$ controls. This was due to an increase in total leukocytes and macrophages in normal air-exposed *Tlr2*$^{-/-}$ controls compared to normal air-exposed WT controls. In contrast, CS-exposed *Tlr4*$^{-/-}$ mice had increased total leukocytes, macrophages, neutrophils and lymphocytes in BALF compared to normal air-exposed *Tlr4*$^{-/-}$ controls. Importantly, total leukocytes, macrophages, neutrophils and lymphocytes in BALF were not significantly altered in CS-exposed *Tlr2*$^{-/-}$ or *Tlr4*$^{-/-}$ mice compared to CS-exposed WT controls.

We then assessed inflammatory cell numbers in the parenchymal histology. CS exposure of WT mice significantly increased inflammatory cell numbers in the parenchyma compared to normal air-exposed WT controls (Figure 5E). CS-exposed *Tlr2*$^{-/-}$ and *Tlr4*$^{-/-}$ mice also had increased parenchymal inflammatory cells compared to their respective normal air-exposed controls and were not significantly different from CS-exposed WT controls.

Next, histopathology was scored according to a set of custom-designed criteria as described previously (40, 44). CS exposure of WT mice increased histopathology score (Figure 5F), which was characterized by increased airway, vascular and parenchymal

inflammation (Figure 5G-I). CS-exposed *Tlr2*$^{-/-}$ and *Tlr4*$^{-/-}$ mice also had increased histopathology, airway, vascular and parenchymal inflammation scores compared to their respective normal air-exposed controls. Representative images are shown in Figure 5J. *Tlr2*$^{-/-}$, but not *Tlr4*$^{-/-}$ mice had a small but significantly increased total histopathology score compared to CS-exposed WT controls, which was characterized by increased parenchymal inflammation score. Normal air-exposed *Tlr2*$^{-/-}$, but not *Tlr4*$^{-/-}$ mice also had a small increase in vascular and parenchymal inflammation scores compared to normal air-exposed WT mice.

We then profiled the mRNA expression of the pro-inflammatory cytokine TNFα, chemokine (C-X-C motif) ligand (CXCL)1, chemokine (C-C motif) ligands (CCL)2, CCL3, CCL4, CCL12, CCL22 and COPD-related factors matrix metalloproteinase (MMP)-12 and serum amyloid A3 (SAA3, Figure 6A-I). CS exposure induced this cytokine, and these chemokines and factors in WT, *Tlr2*$^{-/-}$ and *Tlr4*$^{-/-}$ mice. However, some were not altered in CS-exposed *Tlr2*$^{-/-}$ and/or *Tlr4*$^{-/-}$ mice compared to CS-exposed WT controls, whilst others showed differences (e.g. increased TNFα, CXCL1, CCL2, CCL12 and CCL22 in CS-exposed *Tlr4*$^{-/-}$ mice compared to CS-exposed WT controls) in expression but were not consistent with the inflammatory cell profile (Figure 5) observed in CS-exposed *Tlr2*$^{-/-}$ and *Tlr4*$^{-/-}$ mice compared to CS-exposed WT controls. Notably, however, the mRNA expression of the pro-fibrotic and emphysema factor MMP-12 (Figure 6H) was significantly reduced in CS-exposed *Tlr4*$^{-/-}$ mice compared to CS-exposed WT controls.

Given that TLR2 and TLR4 have been previously shown to play roles in mediating pulmonary oxidative stress (32, 61, 83, 109), we also profiled the mRNA expression of NADPH oxidase (Nox)1, Nox2, Nox3, Nox4, NAD(P)H quinone dehydrogenase (Nqo)1, nuclear factor (erythroid-derived 2)-like-2 factor (Nrf2), glutamate-cysteine ligase catalytic subunit (Gclc), glutathione peroxidase (Gpx)2, heme oxygenase (Hmox)1 and glutathione S-transferase pi (Gstp)1 (Figure 6J-S). CS exposure induced the expression of Nox2 (Figure

6K) and suppressed Gstp1 (Figure 6S), whilst other genes were not altered in *Tlr2*$^{-/-}$ or *Tlr4*$^{-/-}$ mice compared to WT controls. Interestingly, Nox3 (Figure 6L) was increased in normal air-exposed *Tlr4*$^{-/-}$ mice compared to normal air-exposed WT controls, but was reduced by CS exposure. Other oxidative stress-associated genes were, however, not significantly altered in normal air-exposed *Tlr2*$^{-/-}$ or *Tlr4*$^{-/-}$ mice compared to normal air-exposed WT controls.

To determine whether the TNFα signaling pathway was altered in CS-exposed *Tlr4*$^{-/-}$ mice, we next assessed the levels of TNFα protein in lung homogenates. As expected, TNFα protein levels were increased in CS-exposed WT mice compared to normal air-exposed WT controls (Figure 6T). In contrast, TNFα protein levels were not altered in CS-exposed *Tlr2*$^{-/-}$ and *Tlr4*$^{-/-}$ mice compared to normal air-exposed *Tlr2*$^{-/-}$ and *Tlr4*$^{-/-}$ mice, respectively. The lack of increase in CS-exposed *Tlr2*$^{-/-}$ mice was due to increased TNFα levels in normal air-exposed *Tlr2*$^{-/-}$ mice compared normal air-exposed WT mice. Notably, TNFα protein was significantly reduced in CS-exposed *Tlr4*$^{-/-}$ mice compared to CS-exposed WT controls.

CS-induced Collagen Deposition is not Altered in TLR2-deficeint Mice but Completely Attenuated in TLR4-deficient Mice with Experimental COPD

We have previously shown that mice develop small airway remodeling and fibrosis in experimental COPD (7, 40, 41, 62). In agreement with this, CS exposure of WT mice increased small airway epithelial cell area (epithelial thickening) compared to normal air-exposed WT controls (Figure 7A). CS-exposed *Tlr2*$^{-/-}$ and *Tlr4*$^{-/-}$ mice also had increased small airway epithelial cell thickening compared to their respective normal air-exposed controls, but were not altered compared to CS-exposed WT controls. CS-induced small airway epithelial cell thickening in WT, *Tlr2*$^{-/-}$ and *Tlr4*$^{-/-}$ mice was associated with increased numbers of nuclei in the small airways, which is an indicator of increased numbers of

epithelial cells (Figure 7B). The numbers of nuclei in CS-exposed *Tlr2*$^{-/-}$ and *Tlr4*$^{-/-}$ mice were not altered compared to CS-exposed WT controls.

We next assessed airway fibrosis in terms of collagen deposition around small airways. As expected, CS-exposed WT mice had increased collagen deposition compared to normal air-exposed WT controls (Figure 7C). However, CS-exposed *Tlr2*$^{-/-}$ and *Tlr4*$^{-/-}$ mice did not have increased collagen deposition compared to their respective normal air-exposed controls. The former was due to an increase in collagen deposition in normal air-exposed *Tlr2*$^{-/-}$ mice compared normal air-exposed WT controls. The latter was due to no increase in collagen deposition in CS-exposed *Tlr4*$^{-/-}$ mice compared to normal air-exposed *Tlr4*$^{-/-}$ controls. Notably, CS-induced collagen deposition was attenuated in CS-exposed *Tlr4*$^{-/-}$ mice compared to CS-exposed WT controls. This was associated with a concomitant increase in the levels of hyaluronan in BALF and decrease in fibronectin mRNA expression in lung homogenates of *Tlr4*$^{-/-}$ mice compared to WT mice, independent of CS exposure (Figure 7D-E). Notably, CS-induced expression of IL-33 mRNA was also attenuated in *Tlr4*$^{-/-}$ mice (Figure 7F).

CS-induced Emphysema-like Alveolar Enlargement, Apoptosis and Lung Function Impairment are Increased in TLR2-deficient Mice and Decreased in TLR4-deficient Mice with Experimental COPD

We have previously shown that CS-exposed WT mice developed emphysema-like alveolar enlargement and impaired lung function after 8 weeks of CS exposure (7, 40, 41, 62). Thus, we next sought to determine whether TLR2 and TLR4 contribute to these disease features. In agreement with our previous studies, CS-exposed WT mice had significantly increased alveolar septal damage and diameter, determined by destructive index and mean linear

intercept techniques respectively, compared to normal air-exposed WT controls (Figure 8A-B). CS-exposed *Tlr2*$^{-/-}$ and *Tlr4*$^{-/-}$ mice also had increased alveolar septal damage and alveolar diameter compared to normal air-exposed *Tlr2*$^{-/-}$ and *Tlr4*$^{-/-}$ controls, respectively. However, CS-exposed *Tlr2*$^{-/-}$ mice had increased alveolar damage and diameter compared to CS-exposed WT controls. Conversely, CS-exposed *Tlr4*$^{-/-}$ mice had reduced alveolar septal damage and diameter compared to CS-exposed WT controls.

We have previously shown that increased CS-induced emphysema-like alveolar enlargement was associated with increased numbers of TUNEL^{+} cells in the parenchyma, which indicates increased apoptosis (41). In agreement with this, CS-exposed WT mice had increased TUNEL^{+} cells in the parenchyma compared to normal air-exposed WT controls (Figure 8C). CS-exposed *Tlr2*$^{-/-}$ mice had increased TUNEL^{+} cells in the parenchyma compared to normal air-exposed *Tlr2*$^{-/-}$ controls. Importantly, and in agreement with the reduced emphysema-like alveolar enlargement, CS-exposed *Tlr4*$^{-/-}$ mice did not have increased apoptosis compared to normal air-exposed *Tlr4*$^{-/-}$ controls. Accordingly, the numbers of TUNEL^{+} cells were increased in CS-exposed *Tlr2*$^{-/-}$ mice, but reduced significantly in CS-exposed *Tlr4*$^{-/-}$ mice compared to CS-exposed WT controls.

To provide further evidence for changes in apoptosis, we also assessed the levels of active caspase-3, a key molecular marker of apoptosis (19, 34, 79), in whole lung sections by immunohistochemistry. Caspase-3 levels were increased in the lung parenchyma of CS-exposed WT mice compared to normal air-exposed WT controls (Figure 8D). Caspase-3 was also increased in the lung parenchyma of CS-exposed *Tlr2*$^{-/-}$ mice compared to normal air-exposed *Tlr2*$^{-/-}$ controls. In contrast, caspase-3 levels were not altered in CS-exposed *Tlr4*$^{-/-}$ mice compared to normal air-exposed *Tlr4*$^{-/-}$ controls. Notably, the levels of caspase-3 were increased in CS-exposed *Tlr2*$^{-/-}$ mice but were significantly reduced in CS-exposed *Tlr4*$^{-/-}$ mice compared to CS-exposed WT mice.

439 We next assessed the roles of TLR2 and TLR4 in CS-induced impairment of lung
440 function, measured in terms of TLC and transpulmonary resistance. As expected, CS-exposed
441 WT mice had increased TLC (Figure 8E) and transpulmonary resistance (Figure 8F)
442 compared to normal air-exposed WT controls. CS-exposed *Tlr2*$^{-/-}$ mice did not have altered
443 TLC compared to normal air-exposed *Tlr2*$^{-/-}$ controls. This was due to increased TLC in
444 normal air-exposed *Tlr2*$^{-/-}$ mice compared to normal air-exposed WT controls. However, CS-
445 exposed *Tlr2*$^{-/-}$ mice did have increased transpulmonary resistance compared to normal air-
446 exposed *Tlr2*$^{-/-}$ mice. Notably, both TLC and transpulmonary resistance were significantly
447 increased in CS-exposed *Tlr2*$^{-/-}$ mice compared to CS-exposed WT mice. In contrast, *Tlr4*$^{-/-}$
448 mice did not have increases in TLC and transpulmonary resistance compared to normal air-
449 exposed *Tlr4*$^{-/-}$ controls.

450

451 # DISCUSSION

452 In this study, we demonstrate that both TLR2 and TLR4 play important, but opposing
453 roles, in the pathogenesis of CS-induced experimental COPD. TLR2 and TLR4 mRNA were
454 increased in airway epithelium and parenchyma of mice chronically exposed to CS and in
455 human COPD patients. Expression of the co-receptors TLR1, TLR6, CD14 or MD2/Ly96
456 were also increased in CS-exposed mice and human COPD. CS-induced pulmonary
457 inflammation was unaltered in *Tlr2*$^{-/-}$ and *Tlr4*$^{-/-}$ mice compared to WT controls. In contrast,
458 *Tlr2*$^{-/-}$ mice had increased CS-induced emphysema-like alveolar enlargement, apoptosis and
459 impaired lung function, whilst importantly these features were reduced in *Tlr4*$^{-/-}$ mice. CS-
460 induced small airway epithelial thickening and fibrosis were not altered in *Tlr2*$^{-/-}$ mice
461 compared to CS-exposed WT controls. In contrast, CS-induced airway fibrosis, but not small
462 airway epithelial thickening, was significantly attenuated in *Tlr4*$^{-/-}$ mice compared to CS-

463 exposed WT controls. This study provides new insights into the role of TLR2 and TLR4 in
464 the pathogenesis of COPD.

465 The roles of TLR2 and TLR4 in the pathogenesis of COPD are controversial with
466 conflicting data in the literature (3, 21, 22, 30, 33, 65, 66, 69, 75, 80, 85, 87, 91). These
467 conflicting data are likely due to differences between experimental analytes (e.g. peripheral
468 blood monocytes *vs*. macrophages), cohorts of patients with varying medical backgrounds,
469 potential tissue-specificity of TLR expression and the experimental models used (e.g. acute
470 *vs*. chronic CS exposure). Notably, the experimental models utilized either *in vitro*, acute or
471 whole-body CS exposure models, which do not replicate *in vivo* chronic inhaled mainstream
472 CS exposure associated with the induction of COPD in humans (3, 21, 66, 75). Furthermore,
473 these models did not report or demonstrate chronic CS-induced impairment of lung function,
474 which is a key feature of human COPD (7, 31).

475 We aimed to address these discrepancies and delineate the roles of TLR2 and TLR4 in
476 COPD by using an established mouse model of tightly controlled chronic nose-only CS-
477 induced experimental COPD (7, 29, 31, 40, 41, 47, 100). Our models are representative of a
478 pack-a-day smoker and 8 weeks of smoking in a mouse that lives for a year is equivalent to
479 10 years in a human smoker (31, 51). Importantly, we have consistently shown that 8 weeks
480 of CS exposure in our models is sufficient to induce the hallmark features of human COPD:
481 chronic inflammation, airway remodelling, emphysema and impaired lung function (7, 13,
482 16, 29, 31, 40, 41, 47, 100, 102). This 8-week timepoint was specifically chosen to
483 investigate the underlying pathogenic mechanism(s) during the early stages (GOLD I/II) and
484 identify potential therapeutic targets to halt the progression of COPD. Moreover, these
485 shorter-term models may be relevant for testing of therapeutic interventions because new
486 therapeutics such as targeting TLR signaling are likely to have little effect during more severe
487 stages of disease, when invasive interventions, such as lung surgery/transplant, may be

488 required (103). Although there is a possibility that nose-only inhalation murine models of
489 emphysema may introduce other variables such as stress-related to restraint, we observe that
490 mice quickly acclimatize and grew accustomed to our purpose-built restraining tubes (7).
491 This is confirmed by an initial increase in blood corticosterone levels (indicator of stress) in
492 restrained mice during the first week of CS exposure, but these levels return to baseline after
493 that (unpublished data).

494 Interestingly, *Tlr2*$^{-/-}$ mice have not been assessed in the context of CS-induced COPD.
495 *Tlr4*$^{-/-}$ mice on a variety of backgrounds (e.g. C3H/HeJ, C57BL/10ScNJ or C57BL/6J) have
496 been investigated in other CS-exposure models (21, 66), however, *Tlr4*$^{-/-}$ mice on a BALB/c
497 background have not been investigated. Given that MyD88 is the common downstream
498 signaling molecule of all TLRs including both TLR2 and TLR4 (1, 52) we also subjected
499 *MyD88*$^{-/-}$ mice to CS-induced experimental COPD to determine if TLR2- and TLR4-
500 mediated effects were MyD88-dependent. However, these mice became very ill and suffered
501 significant weight loss (>15% body weight) after 3-4 weeks of CS exposure (data not shown).
502 *MyD88*$^{-/-}$ mice are known to be susceptible to opportunistic infections and this was the likely
503 cause of illness in these mice (9, 98).

504 Hence, our study adds to the current literature by investigating the pathogenesis of
505 COPD with previously uninvestigated *Tlr2*$^{-/-}$ and *Tlr4*$^{-/-}$ on a BALB/c background. Moreover,
506 our study also used an established experimental COPD model that utilizes a more clinically
507 relevant CS exposure protocol and is supported by gene expression analysis of published
508 human microarray datasets from healthy non-smokers and COPD subjects (7, 13, 16, 29, 31,
509 40, 41, 47, 100, 102).

510 We showed that TLR2 mRNA was increased in blunt dissected airways and
511 parenchyma, whereas TLR4 mRNA was increased only in the airways. This suggests that the

512 expression of TLR2 and TLR4 may be tissue-specific within the lung, which may in part
513 explain the discrepancies in the literature on the expression of TLR2 and TLR4 in COPD.
514 Interestingly, the expression of TLR2 and TLR4 were not altered in lung-isolated
515 macrophages from CS-exposed mice. This indicates that CS-induced increases in TLR
516 expression occurs on small airway epithelial cells whilst influxing macrophages may
517 contribute by having constitutive levels of TLR expression and by increasing in numbers.
518 These observations were confirmed with immunohistochemistry that showed that TLR2 and
519 TLR4 expressions were detected on small airway epithelial cells and parenchymal
520 inflammatory cells, which were significantly increased in experimental COPD. Furthermore,
521 subsequent flow cytometry analysis showed CS exposure increased the numbers of TLR2-
522 and/or TLR4-expressing neutrophils and mDCs in the lungs. These results mirror previous
523 studies, by us and others, that showed TLR2 and/or TLR4 are expressed on various cells,
524 including macrophages, peripheral monocytes, neutrophils, mDCs and airway/bronchial
525 epithelial cells in inflammatory disease setting including experimental and human COPD (3,
526 6, 10, 22, 33, 65, 69, 75, 80, 81, 85, 87, 91).

527 Importantly, using pre-existing microarray datasets, we also showed that the
528 expression of TLR2 and TLR4 mRNA was increased in airway epithelial cells from bronchial
529 brushings of patients with mild to moderate COPD. In contrast, TLR2 and TLR4 mRNA
530 were reduced in lung parenchymal cores from patients with severe COPD. Interestingly, a
531 previous human study also described similar observations whereby TLR4 expression was
532 increased in the airway epithelium in mild-to-moderate COPD (FEV_1 >1L) but reduced in
533 severe disease (FEV_1 <1L) (65). Collectively, these data suggest that TLR2 and TLR4
534 expression are increased in the lung parenchyma early in disease in response to CS-exposure,
535 but are reduced in severe COPD patients, which may be due to greater tissue destruction that

results in the loss of tissues/cells expressing these TLRs. This also may explain the current discrepancies in the literature on the expression of TLR2 and TLR4 in COPD.

Others have shown that TLR1 and TLR6 were increased on $CD8^+$ T cells from COPD patients (30), and that CD14 levels were increased by CS and associated with impaired lung function in smokers (17, 110). It has been reported that MD2 expression was unaltered in small airway epithelium, but was reduced in the large airways of smokers and patients with stable COPD (74). These data suggest that the effects of CS on the expression of TLR2 and TLR4 co-receptors may also be tissue- or cell-specific (e.g. airway epithelium *vs*. inflammatory cells) and dependent on the severity of the disease. Thus, ligation of TLR2 and TLR4 with their co-receptors may also partially explain the discrepancies in the current literature.

In contrast to our observations in *Tlr2*$^{-/-}$ mice, previous studies showed that inhibition of TLR2 reduced pulmonary inflammation, apoptosis and lung function impairment in other chronic lung diseases, including pulmonary fibrosis and asthma (59, 106). Mice deficient in TLR2 or treated with a neutralizing antibody had reduced bleomycin-induced pulmonary inflammation, collagen deposition and hydroxyproline levels in the lungs (106). Moreover, *Tlr2*$^{-/-}$ mice had reduced airway inflammation and peri-bronchial collagen deposition in an OVA-induced model of experimental allergic asthma (59). In addition, TLR2 was shown to promote apoptosis in human kidney epithelial (HEK)-293, human monocytic (THP-1) cells and endothelial cells *in vitro* (2, 81). Ovalbumin-induced airway hyperresponsiveness (AHR) were also previously shown to be reduced in *Tlr2*$^{-/-}$ mice (38, 59). This may be due to differences in pathogenesis, mechanisms and inflammatory cells/responses that may dictate the role of TLR2 in various chronic lung diseases. For example, allergic asthma is dominated by aberrant Th2-type responses typified by increased infiltration of eosinophils and activated mast cells into the airways and increased levels of Th2-associated cytokines such as IL-5 and

IL-13 (44, 45, 95, 96). In contrast, COPD is typically associated with Th1/Th17-type inflammatory responses characterized by infiltration of macrophages, neutrophils and cytotoxic T cells and the production of Th1/Th17-associated cytokines such as IFN-γ and IL-17A (7, 30, 69, 80, 91). Hence, the role of TLR2 in different chronic lung diseases may largely depend on the presence and type of specific TLR2-expressing cells. Nevertheless, our studies suggest that TLR2 may potentially have a protective role in CS-induced COPD. The underlying mechanism remained unclear, but appeared to be independent of oxidative stress in the lung.

Interestingly, inflammatory infiltrates in the airway lumen and around blood vessels, TNFα protein and TLC were increased in normal air-exposed *Tlr2*$^{-/-}$ mice compared to WT controls. Previous studies showed that airway inflammation is negatively associated with lung function (4, 8) and may cause lung hyperinflation (increased in TLC) (28, 49, 76). Moreover, increased sputum inflammatory cells (e.g. neutrophils) have been shown to significantly correlate with air trapping in COPD patients (71, 72). Another study showed that TLR2 was highly expressed in human fetal lungs and may be important in regulating the development of this organ (77). Recent studies also have emerged that highlight the importance and interactions of host microbiome, commensal bacteria, infectious exacerbations and TLRs in shaping and regulating immune responses in COPD and other chronic respiratory diseases (11, 14, 15, 43, 68, 89). Taken together, the increased inflammation and TLC observed in normal air-exposed *Tlr2*$^{-/-}$ mice may be a consequence of altered host immune responses, lung development and/or microbiome composition. It is likely that TLR2 and TLR4 will be important in these interactions and during lung development. However, this is outside the scope of this study and will require further work to delineate the relationships.

585 TLR4 has been implicated in CS-induced pulmonary inflammation (21, 66). In other
586 studies, acute (3 days) CS exposure of *Tlr4*$^{-/-}$ mice on a C57BL/6 background resulted in
587 reductions in total inflammatory cells in BALF and lung tissue (21). Sub-acute (5 weeks)
588 exposure of *Tlr4*^{defective} mice also resulted in reduced numbers of BALF total inflammatory
589 cells compared to WT C3H/HeJ controls (66). However, in support of our observations, the
590 numbers of BALF total inflammatory cells were not significantly different in these
591 *Tlr4*^{defective} mice compared to WT C3H/HeJ controls following chronic CS exposure (26
592 weeks) (66). Collectively, these suggest TLR4 may play only a minor role at the chronic and
593 severe stages of the disease. Whilst CS-exposed *Tlr4*$^{-/-}$ mice had increased pro-inflammatory
594 cytokine TNFα mRNA expression in the lung compared to CS-exposed WT controls, this
595 increase in mRNA expression was in contrast to the significant reduction in TNFα protein
596 levels in CS-exposed *Tlr4*$^{-/-}$ mice. Taken together, these results suggest that there are
597 alterations in the regulation of gene transcriptional and post-translational protein production
598 in CS-exposed *Tlr4*$^{-/-}$ mice, which collectively does not affect airway or parenchymal
599 inflammation. The biology of these changes is not understood.

600 We previously showed that parenchymal inflammatory cells and alveolar destruction
601 were further increased in WT mice after 12 weeks of CS compared to those exposed to CS
602 for 8 weeks (7). Hence, increasing CS exposure time in mice (e.g. from 8 to 12 weeks) may
603 lead to further alterations in inflammatory gene expression and inflammation. However,
604 given that TLR2 and TLR4 expression were reduced in lung parenchymal cores from severe
605 (GOLD III/IV) COPD patients (Figure 2), we speculate that increasing CS exposure time to
606 induce more severe disease in our model may have similar effects and promote further loss of
607 tissue/cells expressing TLR2 and/or TLR4. In support of this, a previous human study also
608 found that TLR4 expression was inversely proportional to COPD severity (65). Moreover, we
609 also showed that the expression of pro-inflammatory TNFα and chemokine CXCL1 were not

610 increased further with longer exposures, despite increases in parenchymal inflammatory cells,
611 in WT mice exposed to CS for 12 weeks compared to 8 weeks (7). This may be due to some
612 of the functional/molecular changes being restricted to specific cell types (e.g. structural
613 *versus* immune cells) that express TLR2 and/or TLR4 in the lung. Hence, profiling changes
614 in whole lung tissue may have concealed small but potentially critical functional/molecular
615 changes. The roles of TLRs (TLR2 or TLR4) on specific cells in the lungs also remain
616 unclear. This could be addressed in future studies using cell-specific $TLR^{-/-}$ mice or bone
617 marrow chimera studies using $Tlr2^{-/-}$ or $Tlr4^{-/-}$ mice to delineate the role of TLRs on
618 inflammatory *versus* structural cells.

619 CS-induced small airway fibrosis was significantly reduced in lungs of $Tlr4^{-/-}$ mice
620 compared to WT controls. Others have proposed that hyaluronan plays a role in modulating
621 the expression of fibronectin and pulmonary fibrosis in a TLR4-dependent manner (50, 107).
622 Moreover, IL-33 is known to be a pro-fibrotic factor and has been shown to be important in
623 chronic lung diseases, including COPD and asthma (20, 84, 105). Thus, the reduction in
624 small airway fibrosis in $Tlr4^{-/-}$ mice may result from the impairment of the effects of
625 hyaluronan in BALF and IL-33 and fibronectin in the lungs. TLR4 also plays a critical role in
626 bleomycin-induced pulmonary fibrosis (42, 58, 60, 86). TLR4 mRNA expression was
627 increased in mice administered with bleomycin (58), and $Tlr4^{-/-}$ mice were protected against
628 bleomycin-induced pulmonary fibrosis (increased lung collagen levels) and mortality (60).
629 Inhibition of TLR4 with an antagonist (E5564) or an inhibitory small hairpin RNA also
630 reduced collagen synthesis and secretion in the lungs (42, 86). Our data further these
631 observations by showing that TLR4 is a mediator of small airway fibrosis induced by CS.

632 Previous studies suggest that mice deficient in, or with mutations of, TLR4 on other
633 genetic backgrounds (e.g. C3H/HeJ and C57BL/10ScNJ) developed spontaneous emphysema
634 after 3 months of age in the absence of noxious challenges such as CS (104, 109). This was

635 associated with increased Nox3 expression in lungs of these mice (104, 109). We also
636 observed an increase in Nox3 mRNA in normal air-exposed *Tlr4*$^{-/-}$ BALB/c mice, however,
637 these mice did not develop spontaneous emphysema even at 15-16 weeks of age. In fact,
638 *Tlr4*$^{-/-}$ mice were protected from CS-induced emphysema-like alveolar enlargement, which
639 was associated with reduced apoptosis in the lungs. These findings were supported by the
640 observation of reduced expression of MMP-12, which has been linked to the induction of
641 emphysema (7, 41), and improved lung function in CS-exposed *Tlr4*$^{-/-}$ mice. Moreover, CS
642 exposure appeared to reduce Nox3 mRNA expression in *Tlr4*$^{-/-}$ BALB/c mice back to levels
643 observed in normal air-exposed WT BALB/c mice.

644 The differences in genetic background may account for the conflicting results. For
645 example, spontaneous chronic lung disease (severe lung inflammation, increased collagen
646 deposition and alveolar wall thickening) only manifest in Src homology 2 domain–containing
647 inositol-5-phosphatase 1 (SHIP-1)-deficient mice on C57BL/6, but not BALB/c, background
648 (23, 67). In the context of human COPD, this may be important as the severity of the disease
649 in humans often varies between individuals and genetic make-up in combination with
650 environmental exposures are critical. These observations highlight the potential importance
651 of genetic factors in predisposing certain individuals to COPD. This is clinically relevant as
652 only 50% of life-long smokers developed COPD (64). Importantly, this may also indicate that
653 certain individuals may respond better to TLR-based interventions such as Eritoran (currently
654 in phase 3 clinical trial (73)). Eritoran is a synthetic TLR4 antagonist and was shown to
655 protect mice against acute lethal influenza infection (88).

656 Our study demonstrates a previously unrecognized protective role for TLR2 in the
657 pathogenesis of COPD. This supports current evidence in the literature that shows a loss-of-
658 function polymorphism in the TLR2, but not TLR4, gene is associated with accelerated lung
659 function declines in COPD patients (12). TLR2 polymorphisms also predispose patients with

other chronic lung diseases (e.g. cystic fibrosis) to rapid lung function decline (35). This further highlights the potential protective role of TLR2 in chronic lung diseases, and screening for TLR2 polymorphisms may be useful in the prognosis of COPD patients. Furthermore, using a clinically-relevant and established model of CS-induced COPD, our study demonstrates that TLR4 promotes CS-induced airway fibrosis, apoptosis, emphysema-like alveolar enlargement and lung function impairment. Hence, activating TLR2 and/or inhibiting TLR4 may be potential therapeutic strategies in COPD.

ACKNOWLEDGEMENTS

This study was supported by grants from the National Health and Medical Research Council (NHMRC) of Australia and the Australian Research Council (ARC). M.R.S was supported by an NHMRC Early Career Research Fellowship. I.M.A is supported by Wellcome Trust grant. P.M.H was supported by an NHMRC Principal Research Fellowship and by a Brawn Fellowship, Faculty of Health & Medicine, the University of Newcastle. We also would like to thank Kristy Wheeldon, Nathalie Kiaos, Emma Broadfield and staff from the Animal Services Unit of the University of Newcastle and Hunter Medical Research Institute for technical assistance.

COMPETING INTEREST

PMH reports funding/consultancies from Pharmaxis, AstraZeneca, Sanofi, Pharmakea, Ausbio, and Allakos outside the submitted work. Other authors declared no conflict of interest, financial or otherwise.

REFERENCES

1. **Akira S**, **Takeda K**. Toll-like receptor signalling. *Nat Rev Immunol* 4: 499–511, 2004.
2. **Aliprantis AO**, **Yang RB**, **Weiss DS**, **Godowski P**, **Zychlinsky A**. The apoptotic signaling pathway activated by Toll-like receptor-2. *EMBO J* 19: 3325–3336, 2000.
3. **An CH**, **Wang XM**, **Lam HC**, **Ifedigbo E**, **Washko GR**, **Ryter SW**, **Choi AMK**. TLR4 deficiency promotes autophagy during cigarette smoke-induced pulmonary emphysema. *AJP Lung Cell Mol Physiol* 303: L748–L757, 2012.
4. **Baraldo S**, **Turato G**, **Badin C**, **Bazzan E**, **Beghé B**, **Zuin R**, **Calabrese F**, **Casoni G**, **Maestrelli P**, **Papi A**, **Fabbri LM**, **Saetta M**. Neutrophilic infiltration within the airway smooth muscle in patients with COPD. *Thorax* 59: 308–12, 2004.
5. **Barnes PJ**. Corticosteroid resistance in patients with asthma and chronic obstructive pulmonary disease. *J Allergy Clin Immunol* 131: 636–645, 2013.
6. **Beckett EL**, **Phipps S**, **Starkey MR**, **Horvat JC**, **Beagley KW**, **Foster PS**, **Hansbro PM**. TLR2, but Not TLR4, Is Required for Effective Host Defence against Chlamydia Respiratory Tract Infection in Early Life. *PLoS One* 7: e39460, 2012.
7. **Beckett EL**, **Stevens RL**, **Jarnicki AG**, **Kim RY**, **Hanish I**, **Hansbro NG**, **Deane A**, **Keely S**, **Horvat JC**, **Yang M**, **Oliver BG**, **van Rooijen N**, **Inman MD**, **Adachi R**, **Soberman RJ**, **Hamadi S**, **Wark PA**, **Foster PS**, **Hansbro PM**. A new short-term mouse model of chronic obstructive pulmonary disease identifies a role for mast cell tryptase in pathogenesis. *J Allergy Clin Immunol* 131: 752–62, 2013.
8. **Berger P**, **Laurent F**, **Begueret H**, **Perot V**, **Rouiller R**, **Raherison C**, **Molimard M**, **Marthan R**, **Tunon-de-Lara JM**. Structure and function of small airways in smokers: relationship between air trapping at CT and airway inflammation. *Radiology* 228: 85–94, 2003.
9. **von Bernuth H**, **Picard C**, **Puel A**, **Casanova J-L**. Experimental and natural infections in MyD88- and IRAK-4-deficient mice and humans. *Eur J Immunol* 42: 3126–3135, 2012.
10. **Brunialti MKC**, **Martins PS**, **Barbosa de Carvalho H**, **Machado FR**, **Barbosa LM**, **Salomao R**. TLR2, TLR4, CD14, CD11B, and CD11C expressions on monocytes surface and cytokine production in patients with sepsis, severe sepsis, and septic shock. *Shock* 25: 351–357, 2006.
11. **Budden KF**, **Gellatly SL**, **Wood DLA**, **Cooper MA**, **Morrison M**, **Hugenholtz P**, **Hansbro PM**. Emerging pathogenic links between microbiota and the gut-lung axis. *Nat Rev Microbiol* 15: 55–63, 2017.
12. **Budulac SE**, **Boezen HM**, **Hiemstra PS**, **Lapperre TS**, **Vonk JM**, **Timens W**, **Postma DS**, **GLUCOLD study group**. Toll-like receptor (TLR2 and TLR4) polymorphisms and chronic obstructive pulmonary disease. *PLoS One* 7: e43124, 2012.
13. **Campbell JD**, **McDonough JE**, **Zeskind JE**, **Hackett TL**, **Pechkovsky D V**, **Brandsma C-A**, **Suzuki M**, **Gosselink J V**, **Liu G**, **Alekseyev YO**, **Xiao J**, **Zhang X**, **Hayashi S**, **Cooper JD**, **Timens W**, **Postma DS**, **Knight DA**, **Lenburg ME**, **Hogg**

JC, **Spira A**. A gene expression signature of emphysema-related lung destruction and its reversal by the tripeptide GHK. *Genome Med* 4: 67, 2012.

14. **Chambers DC**, **Gellatly SL**, **Hugenholtz P**, **Hansbro PM**. JTD special edition "Hot Topics in COPD"-The microbiome in COPD. *J Thorac Dis* 6: 1525–31, 2014.

15. **Chotirmall SH**, **Gellatly SL**, **Budden KF**, **Mac Aogáin M**, **Shukla SD**, **Wood DLA**, **Hugenholtz P**, **Pethe K**, **Hansbro PM**. Microbiomes in respiratory health and disease: An Asia-Pacific perspective. *Respirology* 22: 240–250, 2017.

16. **Christenson SA**, **Brandsma C-A**, **Campbell JD**, **Knight DA**, **Pechkovsky D V**, **Hogg JC**, **Timens W**, **Postma DS**, **Lenburg M**, **Spira A**. miR-638 regulates gene expression networks associated with emphysematous lung destruction. *Genome Med* 5: 114, 2013.

17. **Cioe PA**, **Baker J**, **Kojic EM**, **Onen N**, **Hammer J**, **Patel P**, **Kahler CW**. Elevated Soluble CD14 and Lower D-Dimer Are Associated With Cigarette Smoking and Heavy Episodic Alcohol Use in Persons Living With HIV. *JAIDS J Acquir Immune Defic Syndr* 70: 400–405, 2015.

18. **Collison A**, **Hatchwell L**, **Verrills N**, **Wark PAB**, **de Siqueira AP**, **Tooze M**, **Carpenter H**, **Don AS**, **Morris JC**, **Zimmermann N**, **Bartlett NW**, **Rothenberg ME**, **Johnston SL**, **Foster PS**, **Mattes J**. The E3 ubiquitin ligase midline 1 promotes allergen and rhinovirus-induced asthma by inhibiting protein phosphatase 2A activity. *Nat Med* 19: 232–237, 2013.

19. **Demedts IK**, **Demoor T**, **Bracke KR**, **Joos GF**, **Brusselle GG**. Role of apoptosis in the pathogenesis of COPD and pulmonary emphysema. *Respir Res* 7: 53, 2006.

20. **Donovan C**, **Bourke JE**, **Vlahos R**. Targeting the IL-33/IL-13 Axis for Respiratory Viral Infections. *Trends Pharmacol. Sci.* 37: 252–261, 2016.

21. **Doz E**, **Noulin N**, **Boichot E**, **Guenon I**, **Fick L**, **Le Bert M**, **Lagente V**, **Ryffel B**, **Schnyder B**, **Quesniaux VFJ**, **Couillin I**, **Guénon I**, **Fick L**, **Le Bert M**, **Lagente V**, **Ryffel B**, **Schnyder B**, **Quesniaux VFJ**, **Couillin I**. Cigarette Smoke-Induced Pulmonary Inflammation Is TLR4/MyD88 and IL-1R1/MyD88 Signaling Dependent. *J Immunol* 180: 1169–78, 2008.

22. **Droemann D**, **Goldmann T**, **Tiedje T**, **Zabel P**, **Dalhoff K**, **Schaaf B**. Toll-like receptor 2 expression is decreased on alveolar macrophages in cigarette smokers and COPD patients. *Respir Res* 6: 68, 2005.

23. **Duan M**, **Li WC**, **Vlahos R**, **Maxwell MJ**, **Anderson GP**, **Hibbs ML**. Distinct Macrophage Subpopulations Characterize Acute Infection and Chronic Inflammatory Lung Disease. *J Immunol* 189: 946–955, 2012.

24. **Dziarski R**, **Wang Q**, **Miyake K**, **Kirschning CJ**, **Gupta D**. MD-2 Enables Toll-Like Receptor 2 (TLR2)-Mediated Responses to Lipopolysaccharide and Enhances TLR2-Mediated Responses to Gram-Positive and Gram-Negative Bacteria and Their Cell Wall Components. *J Immunol* 166: 1938–1944, 2001.

25. **Eder W**, **Klimecki W**, **Yu L**, **von Mutius E**, **Riedler J**, **Braun-Fahrländer C**, **Nowak D**, **Martinez FD**. Toll-like receptor 2 as a major gene for asthma in children of European farmers. *J Allergy Clin Immunol* 113: 482–488, 2004.

26. **Eidelman DH**, **Ghezzo H**, **Kim WD**, **Cosio MG**. The destructive index and early lung destruction in smokers. *Am Rev Respir Dis* 144: 156–9, 1991.

27. **Essilfie A-T**, **Horvat JC**, **Kim RY**, **Mayall JR**, **Pinkerton JW**, **Beckett EL**, **Starkey MR**, **Simpson JL**, **Foster PS**, **Gibson PG**, **Hansbro PM**. Macrolide therapy suppresses key features of experimental steroid-sensitive and steroid-insensitive asthma. *Thorax* 70: 458–67, 2015.

28. **Ferguson GT**. Why does the lung hyperinflate? *Proc Am Thorac Soc* 3: 176–179, 2006.

29. **Franklin BS**, **Bossaller L**, **De Nardo D**, **Ratter JM**, **Stutz A**, **Engels G**, **Brenker C**, **Nordhoff M**, **Mirandola SR**, **Al-Amoudi A**, **Mangan MS**, **Zimmer S**, **Monks BG**, **Fricke M**, **Schmidt RE**, **Espevik T**, **Jones B**, **Jarnicki AG**, **Hansbro PM**, **Busto P**, **Marshak-Rothstein A**, **Hornemann S**, **Aguzzi A**, **Kastenmüller W**, **Latz E**. The adaptor ASC has extracellular and "prionoid" activities that propagate inflammation. *Nat Immunol* 15: 727–37, 2014.

30. **Freeman CM**, **Martinez FJ**, **Han MK**, **Washko, GR**, **McCubbrey AL**, **Chensue SW**, **Arenberg DA**, **Meldrum CA**, **McCloskey L**, **Curtis JL**, **Washko GR**, **McCubbrey AL**, **Chensue SW**, **Arenberg DA**, **Meldrum CA**, **McCloskey L**, **Curtis JL**. Lung CD8+ T cells in COPD have increased expression of bacterial TLRs. *Respir Res* 14: 13, 2013.

31. **Fricker M**, **Deane A**, **Hansbro PM**. Animal models of chronic obstructive pulmonary disease. *Expert Opin Drug Discov* 9: 629–645, 2014.

32. **Gao F**, **Zhang C**, **Zhou C**, **Sun W**, **Liu X**, **Zhang P**, **Han J**, **Xian L**, **Bai D**, **Liu H**, **Cheng Y**, **Li B**, **Cui J**, **Cai J**, **Liu C**. A critical role of toll-like receptor 2 (TLR2) and its' in vivo ligands in radio-resistance. *Sci Rep* 5: 13004, 2015.

33. **Geraghty P**, **Dabo AJ**, **D'Armiento J**. TLR4 Protein Contributes to Cigarette Smoke-induced Matrix Metalloproteinase-1 (MMP-1) Expression in Chronic Obstructive Pulmonary Disease. *J Biol Chem* 286: 30211–8, 2011.

34. **Geraghty P**, **Wyman AE**, **Garcia-Arcos I**, **Dabo AJ**, **Gadhvi S**, **Foronjy R**. STAT3 modulates cigarette smoke-induced inflammation and protease expression. *Front Physiol* 4: 267, 2013.

35. **Haerynck F**, **Mahachie John JM**, **Van Steen K**, **Schelstraete P**, **Van daele S**, **Loeys B**, **Van Thielen M**, **De Canck I**, **Nuytinck L**, **De Baets F**. Genetic variations in toll-like receptor pathway and lung function decline in Cystic Fibrosis patients. *Hum Immunol* 74: 1649–1655, 2013.

36. **Hallstrand TS**, **Hackett TL**, **Altemeier W a.**, **Matute-Bello G**, **Hansbro PM**, **Knight DA.** Airway epithelial regulation of pulmonary immune homeostasis and inflammation. *Clin Immunol* 151: 1–15, 2014.

37. **Hammad H**, **Chieppa M**, **Perros F**, **Willart MA**, **Germain RN**, **Lambrecht BN**. House dust mite allergen induces asthma via Toll-like receptor 4 triggering of airway structural cells. *Nat Med* 15: 410–6, 2009.

38. **Han M**, **Chung Y**, **Young Hong J**, **Rajput C**, **Lei J**, **Hinde JL**, **Chen Q**, **Weng SP**, **Bentley JK**, **Hershenson MB**. Toll-like receptor 2-expressing macrophages are

required and sufficient for rhinovirus-induced airway inflammation. *J Allergy Clin Immunol* 138: 1619–1630, 2016.

39. **Han MK**, **Agusti A**, **Calverley PM**, **Celli BR**, **Criner G**, **Curtis JL**, **Fabbri LM**, **Goldin JG**, **Jones PW**, **MacNee W**, **Make BJ**, **Rabe KF**, **Rennard SI**, **Sciurba FC**, **Silverman EK**, **Vestbo J**, **Washko GR**, **Wouters EFM**, **Martinez FJ**. Chronic obstructive pulmonary disease phenotypes: The future of COPD. *Am. J. Respir. Crit. Care Med.* 182: 598–604, 2010.

40. **Hansbro PM**, **Hamilton MJ**, **Fricker M**, **Gellatly SL**, **Jarnicki AG**, **Zheng D**, **Frei SM**, **Wong GW**, **Hamadi S**, **Zhou S**, **Foster PS**, **Krilis SA**, **Stevens RL**. Importance of Mast Cell Prss31/Transmembrane Tryptase/Tryptase- in Lung Function and Experimental Chronic Obstructive Pulmonary Disease and Colitis. *J Biol Chem* 289: 18214–18227, 2014.

41. **Haw TJ**, **Starkey MR**, **Nair PM**, **Pavlidis S**, **Liu G**, **Nguyen DH**, **Hsu AC**, **Hanish I**, **Kim RY**, **Collison AM**, **Inman MD**, **Wark PA**, **Foster PS**, **Knight DA**, **Mattes J**, **Yagita H**, **Adcock IM**, **Horvat JC**, **Hansbro PM**. A pathogenic role for tumor necrosis factor-related apoptosis-inducing ligand in chronic obstructive pulmonary disease. *Mucosal Immunol* 9: 859–72, 2016.

42. **He Z**, **Zhu Y**, **Jiang H**. Inhibiting toll-like receptor 4 signaling ameliorates pulmonary fibrosis during acute lung injury induced by lipopolysaccharide: an experimental study. *Respir Res* 10: 126, 2009.

43. **Honda K**, **Littman DR**. The microbiome in infectious disease and inflammation. *Annu Rev Immunol* 30: 759–95, 2012.

44. **Horvat JC**, **Beagley KW**, **Wade MA**, **Preston JA**, **Hansbro NG**, **Hickey DK**, **Kaiko GE**, **Gibson PG**, **Foster PS**, **Hansbro PM**. Neonatal Chlamydial Infection Induces Mixed T-Cell Responses That Drive Allergic Airway Disease. *Am J Respir Crit Care Med* 176: 556–564, 2007.

45. **Horvat JC**, **Starkey MR**, **Kim RY**, **Beagley KW**, **Preston JA**, **Gibson PG**, **Foster PS**, **Hansbro PM**. Chlamydial respiratory infection during allergen sensitization drives neutrophilic allergic airways disease. *J Immunol* 184: 4159–69, 2010.

46. **Hoshino K**, **Takeuchi O**, **Kawai T**, **Sanjo H**, **Ogawa T**, **Takeda Y**, **Takeda K**, **Akira S**. Cutting edge: Toll-like receptor 4 (TLR4)-deficient mice are hyporesponsive to lipopolysaccharide: evidence for TLR4 as the Lps gene product. *J Immunol* 162: 3749–3752, 1999.

47. **Hsu AC-Y**, **Starkey MR**, **Hanish I**, **Parsons K**, **Haw TJ**, **Howland LJ**, **Barr I**, **Mahony JB**, **Foster PS**, **Knight DA**, **Wark PA**, **Hansbro PM**. Targeting PI3K-p110α Suppresses Influenza Virus Infection in Chronic Obstructive Pulmonary Disease. *Am J Respir Crit Care Med* 191: 1012–23, 2015.

48. **Janot L**, **Secher T**, **Torres D**, **Maillet I**, **Pfeilschifter J**, **Quesniaux VFJ**, **Landmann R**, **Ryffel B**, **Erard F**. CD14 works with toll-like receptor 2 to contribute to recognition and control of Listeria monocytogenes infection. *J Infect Dis* 198: 115–24, 2008.

49. **Jeffery PK**. Morphology of the airway wall in asthma and in chronic obstructive pulmonary disease. *Am Rev Respir Dis* 143: 1152–8; discussion 1161, 1991.

50. **Jiang D**, **Liang J**, **Fan J**, **Yu S**, **Chen S**, **Luo Y**, **Prestwich GD**, **Mascarenhas MM**, **Garg HG**, **Quinn DA**, **Homer RJ**, **Goldstein DR**, **Bucala R**, **Lee PJ**, **Medzhitov R**, **Noble PW**. Regulation of lung injury and repair by Toll-like receptors and hyaluronan. *Nat Med* 11: 1173–1179, 2005.

51. **Jones B**, **Donovan C**, **Liu G**, **Gomez HM**, **Chimankar V**, **Harrison CL**, **Wiegman CH**, **Adcock IM**, **Knight DA**, **Hirota JA**, **Hansbro PM**. Animal models of COPD: What do they tell us? *Respirology* 22: 21–32, 2017.

52. **Kawai T**, **Akira S**. The role of pattern-recognition receptors in innate immunity: update on Toll-like receptors. *Nat Immunol* 11: 373–384, 2010.

53. **Kedzierski L**, **Tate MD**, **Hsu AC**, **Kolesnik TB**, **Linossi EM**, **Dagley L**, **Dong Z**, **Freeman S**, **Infusini G**, **Starkey MR**, **Bird NL**, **Chatfield SM**, **Babon JJ**, **Huntington N**, **Belz G**, **Webb A**, **Wark PA**, **Nicola NA**, **Xu J**, **Kedzierska K**, **Hansbro PM**, **Nicholson SE**. Suppressor of Cytokine Signaling (SOCS)5 ameliorates influenza infection via inhibition of EGFR signaling. *Elife* 6, 2017.

54. **Keely S**, **Talley NJ**, **Hansbro PM**. Pulmonary-intestinal cross-talk in mucosal inflammatory disease. *Mucosal Immunol* 5: 7–18, 2012.

55. **Kerkhof M**, **Postma DS**, **Brunekreef B**, **Reijmerink NE**, **Wijga AH**, **de Jongste JC**, **Gehring U**, **Koppelman GH**. Toll-like receptor 2 and 4 genes influence susceptibility to adverse effects of traffic-related air pollution on childhood asthma. *Thorax* 65: 690–697, 2010.

56. **Kim HS**, **Go H**, **Akira S**, **Chung DH**. TLR2-Mediated Production of IL-27 and Chemokines by Respiratory Epithelial Cells Promotes Bleomycin-Induced Pulmonary Fibrosis in Mice. *J Immunol* 187: 4007–4017, 2011.

57. **Kobayashi M**, **Saitoh S-I**, **Tanimura N**, **Takahashi K**, **Kawasaki K**, **Nishijima M**, **Fujimoto Y**, **Fukase K**, **Akashi-Takamura S**, **Miyake K**. Regulatory Roles for MD-2 and TLR4 in Ligand-Induced Receptor Clustering. *J Immunol* 176: 6211–6218, 2006.

58. **Li D**, **Peng L**, **Yuan H**, **Yu L**, **Hua S**. The role of expression of TLR 4 in bleomycin-induced pulmonary fibrosis in mice. *Eur Respir J* 42: P3932-, 2014.

59. **Li X**, **Chen Q**, **Chu C**, **You H**, **Jin M**, **Zhao X**, **Zhu X**, **Zhou W**, **Ji W**. Ovalbumin-induced experimental allergic asthma is Toll-like receptor 2 dependent. *Allergy Asthma Proc* 35: 15–20, 2014.

60. **Li XX**, **Jiang DY**, **Huang XX**, **Guo SL**, **Yuan W**, **Dai HP**. Toll-like receptor 4 promotes fibrosis in bleomycin-induced lung injury in mice. *Genet Mol Res* 14: 17391–8, 2015.

61. **Liu C**, **Zhang C**, **Mitchel REJ**, **Cui J**, **Lin J**, **Yang Y**, **Liu X**, **Cai J**. A critical role of toll-like receptor 4 (TLR4) and its' in vivo ligands in basal radio-resistance. *Cell Death Dis* 4: e649, 2013.

62. **Liu G**, **Cooley MA**, **Jarnicki AG**, **Hsu AC-Y**, **Nair PM**, **Haw TJ**, **Fricker M**, **Gellatly SL**, **Kim RY**, **Inman MD**, **Tjin G**, **Wark PAB**, **Walker MM**, **Horvat JC**, **Oliver BG**, **Argraves WS**, **Knight DA**, **Burgess JK**, **Hansbro PM**. Fibulin-1 regulates the pathogenesis of tissue remodeling in respiratory diseases. *JCI insight* 1: 1–18, 2016.

63. **Lozano R**, **Naghavi M**, **Foreman K**, **Lim S**, **Shibuya K**, **Aboyans V**, **Abraham J**, **Adair T**, **Aggarwal R**, **Ahn SY**, **AlMazroa MA**, **Alvarado M**, **Anderson HR**, **Anderson LM**, **Andrews KG**, **Atkinson C**, **Baddour LM**, **Barker-Collo S**, **Bartels DH**, **Bell ML**, **Benjamin EJ**, **Bennett D**, **Bhalla K**, **Bikbov B**, **Abdulhak A Bin**, **Birbeck G**, **Blyth F**, **Bolliger I**, **Boufous S**, **Bucello C**, **Burch M**, **Burney P**, **Carapetis J**, **Chen H**, **Chou D**, **Chugh SS**, **Coffeng LE**, **Colan SD**, **Colquhoun S**, **Colson KE**, **Condon J**, **Connor MD**, **Cooper LT**, **Corriere M**, **Cortinovis M**, **de Vaccaro KC**, **Couser W**, **Cowie BC**, **Criqui MH**, **Cross M**, **Dabhadkar KC**, **Dahodwala N**, **De Leo D**, **Degenhardt L**, **Delossantos A**, **Denenberg J**, **Des Jarlais DC**, **Dharmaratne SD**, **Dorsey ER**, **Driscoll T**, **Duber H**, **Ebel B**, **Erwin PJ**, **Espindola P**, **Ezzati M**, **Feigin V**, **Flaxman AD**, **Forouzanfar MH**, **Fowkes FGR**, **Franklin R**, **Fransen M**, **Freeman MK**, **Gabriel SE**, **Gakidou E**, **Gaspari F**, **Gillum RF**, **Gonzalez-Medina D**, **Halasa YA**, **Haring D**, **Harrison JE**, **Havmoeller R**, **Hay RJ**, **Hoen B**, **Hotez PJ**, **Hoy D**, **Jacobsen KH**, **James SL**, **Jasrasaria R**, **Jayaraman S**, **Johns N**, **Karthikeyan G**, **Kassebaum N**, **Keren A**, **Khoo J-P**, **Knowlton LM**, **Kobusingye O**, **Koranteng A**, **Krishnamurthi R**, **Lipnick M**, **Lipshultz SE**, **Ohno SL**, **Mabweijano J**, **MacIntyre MF**, **Mallinger L**, **March L**, **Marks GB**, **Marks R**, **Matsumori A**, **Matzopoulos R**, **Mayosi BM**, **McAnulty JH**, **McDermott MM**, **McGrath J**, **Memish ZA**, **Mensah GA**, **Merriman TR**, **Michaud C**, **Miller M**, **Miller TR**, **Mock C**, **Mocumbi AO**, **Mokdad AA**, **Moran A**, **Mulholland K**, **Nair MN**, **Naldi L**, **Narayan KMV**, **Nasseri K**, **Norman P**, **O'Donnell M**, **Omer SB**, **Ortblad K**, **Osborne R**, **Ozgediz D**, **Pahari B**, **Pandian JD**, **Rivero AP**, **Padilla RP**, **Perez-Ruiz F**, **Perico N**, **Phillips D**, **Pierce K**, **Pope CA**, **Porrini E**, **Pourmalek F**, **Raju M**, **Ranganathan D**, **Rehm JT**, **Rein DB**, **Remuzzi G**, **Rivara FP**, **Roberts T**, **De León FR**, **Rosenfeld LC**, **Rushton L**, **Sacco RL**, **Salomon JA**, **Sampson U**, **Sanman E**, **Schwebel DC**, **Segui-Gomez M**, **Shepard DS**, **Singh D**, **Singleton J**, **Sliwa K**, **Smith E**, **Steer A**, **Taylor JA**, **Thomas B**, **Tleyjeh IM**, **Towbin JA**, **Truelsen T**, **Undurraga EA**, **Venketasubramanian N**, **Vijayakumar L**, **Vos T**, **Wagner GR**, **Wang M**, **Wang W**, **Watt K**, **Weinstock MA**, **Weintraub R**, **Wilkinson JD**, **Woolf AD**, **Wulf S**, **Yeh P-H**, **Yip P**, **Zabetian A**, **Zheng Z-J**, **Lopez AD**, **Murray CJ**. Global and regional mortality from 235 causes of death for 20 age groups in 1990 and 2010: a systematic analysis for the Global Burden of Disease Study 2010. *Lancet* 380: 2095–2128, 2012.

64. **Lundbäck B**, **Lindberg A**, **Lindström M**, **Rönmark E**, **Jonsson AC**, **Jönsson E**, **Larsson LG**, **Andersson S**, **Sandström T**, **Larsson K**, **Obstructive Lung Disease in Northern Sweden Studies**. Not 15 but 50% of smokers develop COPD? Report from the Obstructive Lung Disease in Northern Sweden Studies. *Respir Med* 97: 115–22, 2003.

65. **MacRedmond RE**, **Greene CM**, **Dorscheid DR**, **McElvaney NG**, **O'Neill SJ**. Epithelial expression of TLR4 is modulated in COPD and by steroids, salmeterol and cigarette smoke. *Respir Res* 8: 84, 2007.

66. **Maes T**, **Bracke KR**, **Vermaelen KY**, **Demedts IK**, **Joos GF**, **Pauwels RA**, **Brusselle GG**. Murine TLR4 Is Implicated in Cigarette Smoke-Induced Pulmonary Inflammation. *Int Arch Allergy Immunol* 141: 354–368, 2006.

67. **Maxwell MJ**, **Duan M**, **Armes JE**, **Anderson GP**, **Tarlinton DM**, **Hibbs ML**. Genetic segregation of inflammatory lung disease and autoimmune disease severity in SHIP-1-/- mice. *J Immunol* 186: 7164–75, 2011.

68. **McDermott AJ**, **Huffnagle GB**. The microbiome and regulation of mucosal immunity. *Immunology* 142: 24–31, 2014.

69. **Nadigel J**, **Préfontaine D**, **Baglole CJ**, **Maltais F**, **Bourbeau J**, **Eidelman DH**, **Hamid Q**. Cigarette smoke increases TLR4 and TLR9 expression and induces cytokine production from CD8+ T cells in chronic obstructive pulmonary disease. *Respir Res* 12: 149, 2011.

70. **Nair PM**, **Starkey MR**, **Haw TJ**, **Liu G**, **Horvat JC**, **Morris JC**, **Verrills NM**, **Clark AR**, **Ammit AJ**, **Hansbro PM**. Targeting PP2A and proteasome activity ameliorates features of allergic airway disease in mice. *Allergy* 38: 42–49, 2017.

71. **O'Donnell RA**, **Peebles C**, **Ward JA**, **Daraker A**, **Angco G**, **Broberg P**, **Pierrou S**, **Lund J**, **Holgate ST**, **Davies DE**, **Delany DJ**, **Wilson SJ**, **Djukanovic R**. Relationship between peripheral airway dysfunction, airway obstruction, and neutrophilic inflammation in COPD. *Thorax* 59: 837–842, 2004.

72. **O'Donnell R**, **Breen D**, **Wilson S**, **Djukanovic R**. Inflammatory cells in the airways in COPD. *Thorax* 61: 448–54, 2006.

73. **Opal SM**, **Laterre P-F**, **Francois B**, **LaRosa SP**, **Angus DC**, **Mira J-P**, **Wittebole X**, **Dugernier T**, **Perrotin D**, **Tidswell M**, **Jauregui L**, **Krell K**, **Pachl J**, **Takahashi T**, **Peckelsen C**, **Cordasco E**, **Chang C-S**, **Oeyen S**, **Aikawa N**, **Maruyama T**, **Schein R**, **Kalil AC**, **Van Nuffelen M**, **Lynn M**, **Rossignol DP**, **Gogate J**, **Roberts MB**, **Wheeler JL**, **Vincent J-L**, **ACCESS Study Group**. Effect of Eritoran, an Antagonist of MD2-TLR4, on Mortality in Patients With Severe Sepsis. *JAMA* 309: 1154, 2013.

74. **Pace E**, **Ferraro M**, **Chiappara G**, **Vitulo P**, **Pipitone L**, **Di Vincenzo S**, **Gjomarkaj M**. MD2 expression is reduced in large airways of smokers and COPD smokers. *Mol Cell Biochem* 407: 289–297, 2015.

75. **Pace E**, **Ferraro M**, **Siena L**, **Melis M**, **Montalbano AM**, **Johnson M**, **Bonsignore MR**, **Bonsignore G**, **Gjomarkaj M**. Cigarette smoke increases Toll-like receptor 4 and modifies lipopolysaccharide-mediated responses in airway epithelial cells. *Immunology* 124: 401–411, 2008.

76. **Park S-W**, **Park J-S**, **Jeong SH**, **Lee YN**, **Hwangbo Y**, **Park JS**, **Lee JH**, **Jang A-S**, **Kim D-J**, **Uh ST**, **Kim YH**, **Park C-S**. Air trapping is a major determinant of persistent airway obstruction in asthmatics. *Respir Med* 106: 786–793, 2012.

77. **Petrikin JE**, **Gaedigk R**, **Leeder JS**, **Truog WE**. Selective toll-like receptor expression in human fetal lung. *Pediatr Res* 68: 335–338, 2010.

78. **Pinkerton KE**, **Harbaugh M**, **Han MK**, **Jourdan Le Saux C**, **Van Winkle LS**, **Martin WJ**, **Kosgei RJ**, **Carter EJ**, **Sitkin N**, **Smiley-Jewell SM**, **George M**. Women and Lung Disease. Sex Differences and Global Health Disparities. *Am J Respir Crit Care Med* 192: 11–6, 2015.

79. **Plataki M**, **Tzortzaki E**, **Rytila P**, **Demosthenes M**, **Koutsopoulos A**, **Siafakas NM**. Apoptotic mechanisms in the pathogenesis of COPD. *Int J Chron Obstruct Pulmon Dis* 1: 161–71, 2006.

80. **Pons J**, **Sauleda J**, **Regueiro V**, **Santos C**, **Lopez M**, **Ferrer J**, **Agusti AG**, **Bengoechea JA**. Expression of Toll-like receptor 2 is up-regulated in monocytes from patients with chronic obstructive pulmonary disease. *Respir Res* 7: 64, 2006.

81. **Quillard T**, **Araújo HA**, **Franck G**, **Shvartz E**, **Sukhova G**, **Libby P**. TLR2 and neutrophils potentiate endothelial stress, apoptosis and detachment: implications for superficial erosion. *Eur Hear J* 36: 1394–1404, 2015.

82. **Redecke V**, **Häcker H**, **Datta SK**, **Fermin A**, **Pitha PM**, **Broide DH**, **Raz E**. Cutting edge: activation of Toll-like receptor 2 induces a Th2 immune response and promotes experimental asthma. *J Immunol* 172: 2739–43, 2004.

83. **Ruwanpura SM**, **McLeod L**, **Lilja AR**, **Brooks G**, **Dousha LF**, **Seow HJ**, **Bozinovski S**, **Vlahos R**, **Hertzog PJ**, **Anderson GP**, **Jenkins BJ**. Non-essential role for TLR2 and its signaling adaptor Mal/TIRAP in preserving normal lung architecture in mice. *PLoS One* 8: e78095, 2013.

84. **Saglani S**, **Lui S**, **Ullmann N**, **Campbell GA**, **Sherburn RT**, **Mathie SA**, **Denney L**, **Bossley CJ**, **Oates T**, **Walker SA**, **Bush A**, **Lloyd CM**. IL-33 promotes airway remodeling in pediatric patients with severe steroid-resistant asthma. *J Allergy Clin Immunol* 132: 676–685.e13, 2013.

85. **Sarir H**, **Mortaz E**, **Karimi K**, **Kraneveld AD**, **Rahman I**, **Caldenhoven E**, **Nijkamp FP**, **Folkerts G**. Cigarette smoke regulates the expression of TLR4 and IL-8 production by human macrophages. *J Inflamm* 6: 12, 2009.

86. **Savov JD**, **Brass DM**, **Lawson BL**, **McElvania-Tekippe E**, **Walker JKL**, **Schwartz DA**. Toll-like receptor 4 antagonist (E5564) prevents the chronic airway response to inhaled lipopolysaccharide. *Am J Physiol Lung Cell Mol Physiol* 289: L329-37, 2005.

87. **von Scheele I**, **Larsson K**, **Dahlén B**, **Billing B**, **Skedinger M**, **Lantz A-S**, **Palmberg L**. Toll-like receptor expression in smokers with and without COPD. *Respir Med* 105: 1222–1230, 2011.

88. **Shirey KA**, **Lai W**, **Scott AJ**, **Lipsky M**, **Mistry P**, **Pletneva LM**, **Karp CL**, **McAlees J**, **Gioannini TL**, **Weiss J**, **Chen WH**, **Ernst RK**, **Rossignol DP**, **Gusovsky F**, **Blanco JCG**, **Vogel SN**. The TLR4 antagonist Eritoran protects mice from lethal influenza infection. *Nature* 497: 498–502, 2013.

89. **Simpson JL**, **Baines KJ**, **Horvat JC**, **Essilfie A-T**, **Brown AC**, **Tooze M**, **McDonald VM**, **Gibson PG**, **Hansbro PM**. COPD is characterized by increased detection of Haemophilus influenzae, Streptococcus pneumoniae and a deficiency of Bacillus species. *Respirology* 21: 697–704, 2016.

90. **Simpson JL**, **Grissell TV**, **Douwes J**, **Scott RJ**, **Boyle MJ**, **Gibson PG**. Innate immune activation in neutrophilic asthma and bronchiectasis. *Thorax* 62: 211–218, 2007.

91. **Simpson JL**, **McDonald VM**, **Baines KJ**, **Oreo KM**, **Wang F**, **Hansbro PM**, **Gibson PG**. Influence of Age, Past Smoking, and Disease Severity on TLR2, Neutrophilic Inflammation, and MMP-9 Levels in COPD. *Mediat Inflamm* 2013: 1–13, 2013.

92. **Simpson JL**, **Powell H**, **Baines KJ**, **Milne D**, **Coxson HO**, **Hansbro PM**, **Gibson PG**. The Effect of Azithromycin in Adults with Stable Neutrophilic COPD: A Double Blind Randomised, Placebo Controlled Trial. *PLoS One* 9: e105609, 2014.

93. **Spina D**. Pharmacology of novel treatments for COPD: are fixed dose combination LABA/LAMA synergistic? *Eur Clin Respir J* 2, 2015.

94. **Starkey MR**, **Essilfie A-T**, **Horvat JC**, **Kim RY**, **Nguyen DH**, **Beagley KW**, **Mattes J**, **Foster PS**, **Hansbro PM**. Constitutive production of IL-13 promotes early-life Chlamydia respiratory infection and allergic airway disease. *Mucosal Immunol* 6: 569–579, 2013.

95. **Starkey MR**, **Kim RY**, **Beckett EL**, **Schilter HC**, **Shim D**, **Essilfie A-T**, **Nguyen DH**, **Beagley KW**, **Mattes J**, **Mackay CR**, **Horvat JC**, **Hansbro PM**. Chlamydia muridarum Lung Infection in Infants Alters Hematopoietic Cells to Promote Allergic Airway Disease in Mice. *PLoS One* 7: e42588, 2012.

96. **Starkey MR**, **Nguyen DH**, **Brown AC**, **Essilfie A-T**, **Kim RY**, **Yagita H**, **Horvat JC**, **Hansbro PM**. Programmed Death Ligand 1 Promotes Early-Life Chlamydia Respiratory Infection-Induced Severe Allergic Airway Disease. *Am J Respir Cell Mol Biol* 54: 493–503, 2016.

97. **Starkey MR**, **Nguyen DH**, **Essilfie A-T**, **Kim RY**, **Hatchwell LM**, **Collison AM**, **Yagita H**, **Foster PS**, **Horvat JC**, **Mattes J**, **Hansbro PM**. Tumor necrosis factor-related apoptosis-inducing ligand translates neonatal respiratory infection into chronic lung disease. *Mucosal Immunol* 7: 478–488, 2014.

98. **Takeuchi O**, **Hoshino K**, **Akira S**. Cutting edge: TLR2-deficient and MyD88-deficient mice are highly susceptible to Staphylococcus aureus infection. *J Immunol* 165: 5392–5396, 2000.

99. **Takeuchi O**, **Hoshino K**, **Kawai T**, **Sanjo H**, **Takada H**, **Ogawa O**, **Takeda K**, **Akira S**. Differential roles of TLR2 and TLR4 in recognition of gram-negative and gram-positive cell wall components. *Immunity* 11: 443–451, 1999.

100. **Tay HL**, **Kaiko GE**, **Plank M**, **Li J**, **Maltby S**, **Essilfie A-T**, **Jarnicki A**, **Yang M**, **Mattes J**, **Hansbro PM**, **Foster PS**. Antagonism of miR-328 increases the antimicrobial function of macrophages and neutrophils and rapid clearance of non-typeable Haemophilus influenzae (NTHi) from infected lung. *PLoS Pathog* 11: e1004549, 2015.

101. **Thorburn AN**, **Foster PS**, **Gibson PG**, **Hansbro PM**. Components of Streptococcus pneumoniae suppress allergic airways disease and NKT cells by inducing regulatory T cells. *J Immunol* 188: 4611–20, 2012.

102. **Tilley AE**, **Harvey B-G**, **Heguy A**, **Hackett NR**, **Wang R**, **O'Connor TP**, **Crystal RG**. Down-regulation of the notch pathway in human airway epithelium in association with smoking and chronic obstructive pulmonary disease. *Am J Respir Crit Care Med* 179: 457–66, 2009.

103. **Vogelmeier CF**, **Criner GJ**, **Martinez FJ**, **Anzueto A**, **Barnes PJ**, **Bourbeau J**, **Celli BR**, **Chen R**, **Decramer M**, **Fabbri LM**, **Frith P**, **Halpin DMG**, **López Varela MV**, **Nishimura M**, **Roche N**, **Rodriguez-Roisin R**, **Sin DD**, **Singh D**, **Stockley R**, **Vestbo J**, **Wedzicha JA**, **Agusti A**. Global Strategy for the Diagnosis, Management, and Prevention of Chronic Obstructive Lung Disease 2017 Report: GOLD Executive Summary. *Am. J. Respir. Crit. Care Med.* (January 27, 2017). doi: 10.1164/rccm.201701-0218PP.

104. **Wang Q**, **Yang H**, **Liu H**, **Mi S**, **Zhang X**, **Yan H**, **Ma Y**, **Wang X**, **Hu Z**. Interleukin-17A is involved in development of spontaneous pulmonary emphysema caused by Toll-like receptor 4 mutation. *Acta Pharmacol Sin* 32: 1045–1054, 2011.

105. **Xia J**, **Zhao J**, **Shang J**, **Li M**, **Zeng Z**, **Zhao J**, **Wang J**, **Xu Y**, **Xie J**. Increased IL-33 expression in chronic obstructive pulmonary disease. *Am J Physiol Lung Cell Mol Physiol* 308: L619-27, 2015.

106. **Yang H-Z**, **Cui B**, **Liu H-Z**, **Chen Z-R**, **Yan H-M**, **Hua F**, **Hu Z-W**. Targeting TLR2 Attenuates Pulmonary Inflammation and Fibrosis by Reversion of Suppressive Immune Microenvironment. *J Immunol* 182: 692–702, 2009.

107. **Yoshizaki A**, **Iwata Y**, **Komura K**, **Ogawa F**, **Hara T**, **Muroi E**, **Takenaka M**, **Shimizu K**, **Hasegawa M**, **Fujimoto M**, **Tedder TF**, **Sato S**. CD19 regulates skin and lung fibrosis via Toll-like receptor signaling in a model of bleomycin-induced scleroderma. *Am J Pathol* 172: 1650–1663, 2008.

108. **Zanoni I**, **Ostuni R**, **Marek LRR**, **Barresi S**, **Barbalat R**, **Barton GMM**, **Granucci F**, **Kagan JCC**. CD14 Controls the LPS-Induced Endocytosis of Toll-like Receptor 4. *Cell* 147: 868–880, 2011.

109. **Zhang X**, **Shan P**, **Jiang G**, **Cohn L**, **Lee PJ**. Toll-like receptor 4 deficiency causes pulmonary emphysema. *J Clin Invest* 116: 3050–3059, 2006.

110. **Zhou H**, **Alexis NE**, **Almond M**, **Donohue J**, **LaForce C**, **Bromberg PA**, **Peden DB**. Influence of C-159T SNP of the CD14 gene promoter on lung function in smokers. *Respir Med* 103: 1358–1365, 2009.

FIGURE LEGENDS

Figure 1. TLR2 and TLR4 mRNA expression and protein levels are increased in CS-induced experimental COPD. Wild-type (WT) BALB/c mice were exposed to normal air or CS and sacrificed after 4, 8 and 12 weeks. (**A**) TLR2 and (**B**) TLR4 mRNA expression in whole lung tissues. (**C**) Muc5ac and Sftpc mRNA expression in blunt dissected airways and parenchyma in normal air-exposed WT mice. (**D-E**) TLR2 and (**F-G**) TLR4 mRNA expression in blunt dissected airways and parenchyma after 8 weeks CS exposure. Muc5ac, Sftpc, TLR2 and TLR4 mRNA expression were normalized to reference gene HPRT and expressed as relative abundance compared to either blunt dissected airways (for Muc5ac and Sftpc mRNA) or normal air-exposed WT controls (for TLR2 and TLR4 mRNA). Immunohistochemistry for (**H-I**) TLR2 and (**J-K**) TLR4 protein on small airway epithelium and lung parenchyma after 8 weeks of CS exposure; scale bars equal 50μm. Arrowheads indicate TLR2 or TLR4 expressing inflammatory cells. Graphs were presented as mean ± SEM and representative from two independent experiments of 6 mice per group. Two-tailed Mann-Whitney t-test analyzed differences between two groups, whereby *$p<0.05$; **$p<0.01$; ***$p<0.001$ compared to normal air-exposed WT controls and #$p<0.05$; ###$p<0.001$ compared to blunt dissected airway.

Figure 2. TLR2- and/or TLR4-expressing neutrophils and mDCs cells were increased in CS-induced experimental COPD. Wild-type (WT) BALB/c mice were exposed to cigarette smoke (CS) or normal air for 8 weeks. (**A**) TLR2 and (**B**) TLR4 mRNA expressions were determined in macrophage isolated from lungs by qPCR. The number of (**C**) $CD11b^+$ monocytes, (**D**) neutrophils and (**E**) myeloid dendritic cells (mDCs) expressing TLR2 and/or TLR4 in lungs. mRNA expressions were normalized to reference gene and expressed as

relative abundance compared to normal air-exposed WT controls. Graphs were presented as mean ± SEM and representative from two independent experiments of 6 mice per group. Two-tailed Mann-Whitney t-test analyzed differences between two groups, whereby *p<0.05; **p<0.01 compared to normal air-exposed WT controls.

Figure 3. TLR2 and TLR4 co-receptor expression are increased in CS-induced experimental COPD. Wild-type (WT) BALB/c mice were exposed to normal air or CS for 8 weeks to induce experimental COPD. (**A-B**) TLR1, (**C-D**) TLR6, (**E-F**) CD14 and (**G-H**) MD2/Ly96 mRNA expressions in blunt dissected airways and parenchyma. mRNA expressions were normalized to reference gene HPRT and expressed as relative abundance compared to normal air-exposed WT controls. Graphs were presented as mean ± SEM and representative from two independent experiments of 6 mice per group. Two-tailed Mann-Whitney t-test analyzed differences between two groups, whereby *p<0.05; **p<0.01; ***p<0.001 compared to normal air-exposed WT controls.

Figure 4. TLR2, TLR4 and co-receptor mRNA expressions are increased in the airways in humans with mild to moderate COPD. Airway epithelial cells were collected from human healthy non-smokers (NS), healthy smokers without COPD (Smoker) and COPD patients with Global Initiative for Chronic Obstructive Lung Disease (GOLD) stage I (Mild) or II (Moderate) disease. (**A**) TLR2, (**B**) TLR4, (**C**) TLR1, (**D**) TLR6, (**E**) CD14 and (**F**) LY96 mRNA expression were assessed by microarray profiling. Lung parenchymal cores were collected from human healthy non-smokers (NS) and COPD patients with Global Initiative for Chronic Obstructive Lung Disease (GOLD) stage IV (severe) disease. (**G**) TLR2, (**H**) TLR4, (**I**) TLR1, (**J**) TLR6 and (**K**) LY96 mRNA expression were assessed by

microarray profiling. Graphs are expressed as log_2 intensity robust multi-array average signals. The Benjamini–Hochberg method for adjusted P value/false discovery rate (FDR) analyzed differences between NS or Smokers and COPD patients.

Figure 5. CS-induced pulmonary inflammation is unaltered in TLR2-deficient and TLR4-deficient mice with experimental COPD. Wild-type (WT), TLR2-deficient (*Tlr2*$^{-/-}$) or TLR4-deficient (*Tlr4*$^{-/-}$) BALB/c mice were exposed to normal air or CS for 8 weeks to induce experimental COPD. (**A**) Total leukocytes, (**B**) macrophages, (**C**) neutrophils and (**D**) lymphocytes were enumerated in May-Grunwald Giemsa stained bronchoalveolar lavage fluid (BALF) cytospin slides. (**E**) The numbers of parenchymal inflammatory cells (arrowheads) were enumerated in periodic acid-Schiff (PAS)-stained lung sections; scale bars equal 20μm. (**F**) Total histopathology score in lung sections and inflammation scores specifically in the (**G**) airway, (**H**) vascular and (**I**) parenchymal regions. **(J)** Representative images of lung histopathology scoring; scale bars equal 50μm. Graphs were presented as mean ± SEM and representative from two independent experiments of 6 mice per group. The one-way analysis of variance with Bonferroni post-test analyzed differences between 3 or more groups, whereby *p<0.05; **p<0.01; ***p<0.001; ****p<0.0001 compared to normal air-exposed WT, *Tlr2*$^{-/-}$ or *Tlr4*$^{-/-}$ controls, #p<0.05; ##p<0.01 compared to CS-exposed WT controls and ϕp<0.05; ϕϕp<0.01; ϕϕϕp<0.001 compared to normal air-exposed WT controls.

Figure 6. Pro-inflammatory cytokine, chemokine, COPD-related factors and oxidative stress-associated gene expressions in CS-induced experimental COPD. Wild-type (WT), TLR2-deficient (*Tlr2*$^{-/-}$) or TLR4-deficient (*Tlr4*$^{-/-}$) BALB/c mice were exposed to normal air or cigarette smoke (CS) for 8 weeks. Pro-inflammatory cytokine (**A**) tumor necrosis factor-α

(TNFα), (**B**) chemokine (C-X-C motif) ligand (CXCL)1, (**C**) chemokine (C-C motif) ligand (CCL)2, (**D**) CCL3, (**E**) CCL4, (**F**) CCL12, (**G**) CCL22, other COPD-related factors; (**H**) matrix metalloproteinase (MMP)-12 and (**I**) serum amyloid A3 (SAA3) mRNA expression were determined in whole lung homogenates by qPCR. Oxidative stress-associated genes (**J**) NADPH oxidase (Nox)1, (**K**) Nox2, (**L**) Nox3, (**M**) Nox4, (**N**) NAD(P)H quinone dehydrogenase (Nqo)1, (**O**) nuclear factor, erythroid 2 like 2 (Nrf2), (**P**) glutamate-cysteine ligase catalytic subunit (Gclc), (**Q**) glutathione peroxidase (Gpx)2, (**R**) heme oxygenase (Hmox)1 and (**S**) glutathione S-transferase pi (Gstp)1 expression were determined in whole lung homogenates by qPCR. mRNA expression was normalized to the reference gene HPRT and expressed as relative abundance compared to normal air-exposed WT controls. (**T**) The levels of TNFα protein in lung homogenates were determined by ELISA and normalized to total protein. Graphs were presented as mean ± SEM and representative from two independent experiments of 6 mice per group. The one-way analysis of variance with Bonferroni post-test was used to analyze differences between 3 or more groups, whereby *p<0.05; **p<0.01; ***p<0.001; ****p<0.0001 compared to normal air-exposed WT, *Tlr2*$^{-/-}$ or *Tlr4*$^{-/-}$ controls, #p<0.05; ##p<0.01; ###p<0.001; ####p<0.0001 compared to CS-exposed WT controls, ϕp<0.05; ϕϕϕϕp<0.0001 compared normal air-exposed WT controls and *ns* denotes not significant.

Figure 7. CS-induced airway remodeling and fibrosis is not altered in TLR2-deficient mice whilst CS-induced airway fibrosis, but not remodeling, is completely attenuated in TLR4-deficient mice with experimental COPD. Wild-type (WT), TLR2-deficient (*Tlr2*$^{-/-}$) or TLR4-deficient (*Tlr4*$^{-/-}$) BALB/c mice were exposed to normal air or CS for 8 weeks to induce experimental COPD. (**A**) Small airway epithelial thickness in terms of epithelial cell area (μm^2) per basement membrane (BM) perimeter (μm) was determined in periodic acid-

Schiff (PAS)-stained whole lung sections; scale bars equal 50μm. (**B**) The number of epithelial cells in PAS-stained lung sections was assessed by enumerating the number of nuclei per 100μm of BM perimeter; scale bars equal 20μm. (**C**) Area of collagen deposition (μm^2) per BM perimeter (μm) was determined in Masson's Trichrome-stained lung sections; scale bars equal 200μm. Inserts show expanded images of indicated regions; scale bars equal 200μm). (**D**) The level of hyaluronan in BALF was determined by ELISA. The mRNA expression of (**E**) fibronectin and (**F**) interleukin (IL)-33 were determined in whole lung homogenates by qPCR. mRNA expression was normalized to the reference gene HPRT and expressed as relative abundance compared to normal air-exposed WT controls. Graphs were presented as mean ± SEM and representative from two independent experiments of 6 mice per group. The one-way analysis of variance with Bonferroni post-test analyzed differences between 3 or more groups, whereby *p<0.05; **p<0.01; ***p<0.001; ****p<0.0001 compared to normal air-exposed WT, *Tlr2*$^{-/-}$ or *Tlr4*$^{-/-}$ controls, #p<0.05; ##p<0.01; ####p<0.0001 compared to CS-exposed WT controls, ϕp<0.05; ϕϕϕϕp<0.0001 compared to normal air-exposed WT controls and *ns* denotes not significant.

Figure 8. CS-induced emphysema-like alveolar enlargement, apoptosis and impaired lung function are increased in TLR2-deficient mice and decreased in TLR4-deficient mice with experimental COPD. Wild-type (WT), TLR2-deficient (*Tlr2*$^{-/-}$) or TLR4-deficient (*Tlr4*$^{-/-}$) BALB/c mice were exposed to normal air or CS for 8 weeks to induce experimental COPD. (**A**) Alveolar septal damage and (**B**) diameter (μm) were determined in H&E-stained lung sections using destructive index and mean linear intercept techniques respectively; scale bars equal 50μm. (**C**) The numbers of TUNEL^{+} cells (arrowheads) were enumerated in whole lung sections at high power field (HPF; 100x); scale bars equal 20μm. Immunohistochemistry for (**D**) active caspase-3 protein on lung parenchyma after 8 weeks of

CS exposure; scale bars equal 50μm. Arrowheads indicate caspase-3-expressing alveolar septa cells. Lung function was assessed in terms of (**E**) total lung capacity (TLC) and (**F**) transpulmonary resistance. Graphs were presented as mean ± SEM and representative from two independent experiments of 6 mice per group. The one-way analysis of variance with Bonferroni post-test analyzed differences between 3 or more groups, whereby **p<0.01; ***p<0.001; ****p<0.0001 compared to normal air-exposed WT, *Tlr2*$^{-/-}$ or *Tlr4*$^{-/-}$ controls, #p<0.05; ##p<0.01; ####p<0.0001 compared to CS-exposed WT controls, ϕϕϕϕp<0.0001 compared to normal air-exposed WT controls and *ns* denotes not significant.

1215 **Table 1.** Custom-designed primers used in qPCR analysis

Primer	Primer sequence (5' → 3')
TLR2 forward	TGTAGGGGCTTCACTTCTCTGCTT
TLR2 reverse	AGACTCCTGAGCAGAACAGCGTTT
TLR4 forward	TGGTTGCAGAAAATGCCAGG
TLR4 reverse	GGAACTACCTCTATGCAGGGAT
Muc5ac forward	GCAGTTGTGTCACCATCATCTGTG
Muc5ac reverse	GGGGCAGTCTTGACTAACCCTCTT
Sftpc forward	TGTATGACTACCAGCGGCTC
Sftpc reverse	AGCGAAAGCCTCAAGACTAGG
TNFα forward	TCTGTCTACTGAACTTCGGGGTGA
TNFα reverse	TTGTCTTTGAGATCCATGCCGTT
CXCL1 forward	GCTGGGATTCACCTCAAGAA
CXCL1 reverse	CTTGGGGACACCTTTTAGCA
CCL2 forward	TGAGTAGCAGCAGGTGAGTGGGG
CCL2 reverse	TGTTCACAGTTGCCGGCTGGAG
CCL3 forward	CTCCCAGCCAGGTGTCATTTT
CCL3 reverse	CTTGGACCCAGGTCTCTTTGG
CCL4 forward	GTGGCTGCCTTCTGTGCTCCA
CCL4 reverse	AGCTGCCGGGAGGTGTAAGAGAA
CCL12 forward	CCGGGAGCTGTGATCTTCA
CCL12 reverse	AACCCACTTCTCGGGGT
CCL22 forward	TGGCTACCCTGCGTCGTGTCCCA
CCL22 reverse	CGTGATGGCAGAGGGTGACGG
MMP-12 forward	CCTCGATGTGGAGTGCCCGA
MMP-12 reverse	CCTCACGCTTCATGTCCGGAG
SAA3 forward	TGATCCTGGGAGTTGACAGCCAA
SAA3 reverse	ACCCCTCCGGGCAGCATCATA
Nox1 forward	CCCCTGAGTCTTGGAAGTGG
Nox1 reverse	GGGTGCATGACAACCTTGGTA
Nox2 forward	AACTGGGCTGTGAATGAAGG
Nox2 reverse	CAGCAGGATCAGCATACAGTTG

Nox3 forward	CTCGTTGCCTACGGGATAGC
Nox3 reverse	CCTTCAGCATCCTTGGCCT
Nox4 forward	ACAACCAAGGGCCAGAATACTACTAC
Nox4 reverse	GGATGAGGCTGCAGTTGAGG
Nqo1 forward	GTAGCGGCTCCATGTACTCTC
Nqo1 reverse	AGGATGCCACTCTGAATCGG
Nrf2 forward	CTTTAGTCAGCGACAGAAGGAC
Nrf2 reverse	AGGCATCTTGTTTGGGAATGTG
Gclc forward	CGACCAATGGAGGTGCAGTTA
Gclc reverse	AACCTTGGACAGCGGAATGA
Gpx2 forward	ACCAGTTCGGACATCAGGAG
Gpx2 reverse	CCCAGGTCGGACATACTTGA
Hmox1 forward	GGTGCAAGATACTGCCCCTG
Hmox1 reverse	TGAGGACCCACTGGAGGAG
Gstp1 forward	GGCATGCCACCATACACCAT
Gstp1 reverse	ATTCGCATGGCCTCACACC
Fibronectin forward	TGTGGTTGCCTTGCACGAT
Fibronectin reverse	GCTATCCACTGGGCAGTAAAGC
IL-33 forward	CCTCCCTGAGTACATACAATGACC
IL-33 reverse	GTAGTAGCACCTGGTCTTGCTCTT
HPRT forward	AGGCCAGACTTTGTTGGATTTGAA
HPRT reverse	CAACTTGCGCTCATCTTAGGATTT

1216

1217

1218 **Table 2.** Surface antigens used to characterize mouse lung cell subsets by flow cytometry

Cell subset	Cell surface antigens
$CD11b^+$ monocyte	$CD45^+$ $F4/80^+$ $CD11c^-$ $CD11b^+$ $Ly6C^+$ $TLR2^{+/-}$ $TLR4^{+/-}$
Neutrophil	$CD45^+$ $F4/80^-$ $CD11b^+$ $Ly6G^+$ $TLR2^{+/-}$ $TLR4^{+/-}$
Myeloid dendritic cell	$CD45^+$ $F4/80^-$ $CD11c^+$ $CD11b^+$ $MHCII^+$ $TLR2^{+/-}$ $TLR4^{+/-}$

1219

1220

1221 **Table 3.** Antibodies used in flow cytometry analysis

Cell surface antigens	Clone	Fluorophore	Company
CD45	30-F11	AF-700	Biolegend
F4/80	T45-2342	BV711	BD Biosciences
CD11c	HL3	BV421	BD Biosciences
CD11b	M1/70	PerCPCy5.5	Biolegend
Ly6G	1A8	BV510	Biolegend
MHCII	M5/114.15.2	APC	Biolegend
TLR2	T2.5	FITC	Biolegend
TLR4	MTS510	PE	BD Biosciences

1222

1223

Figure 1

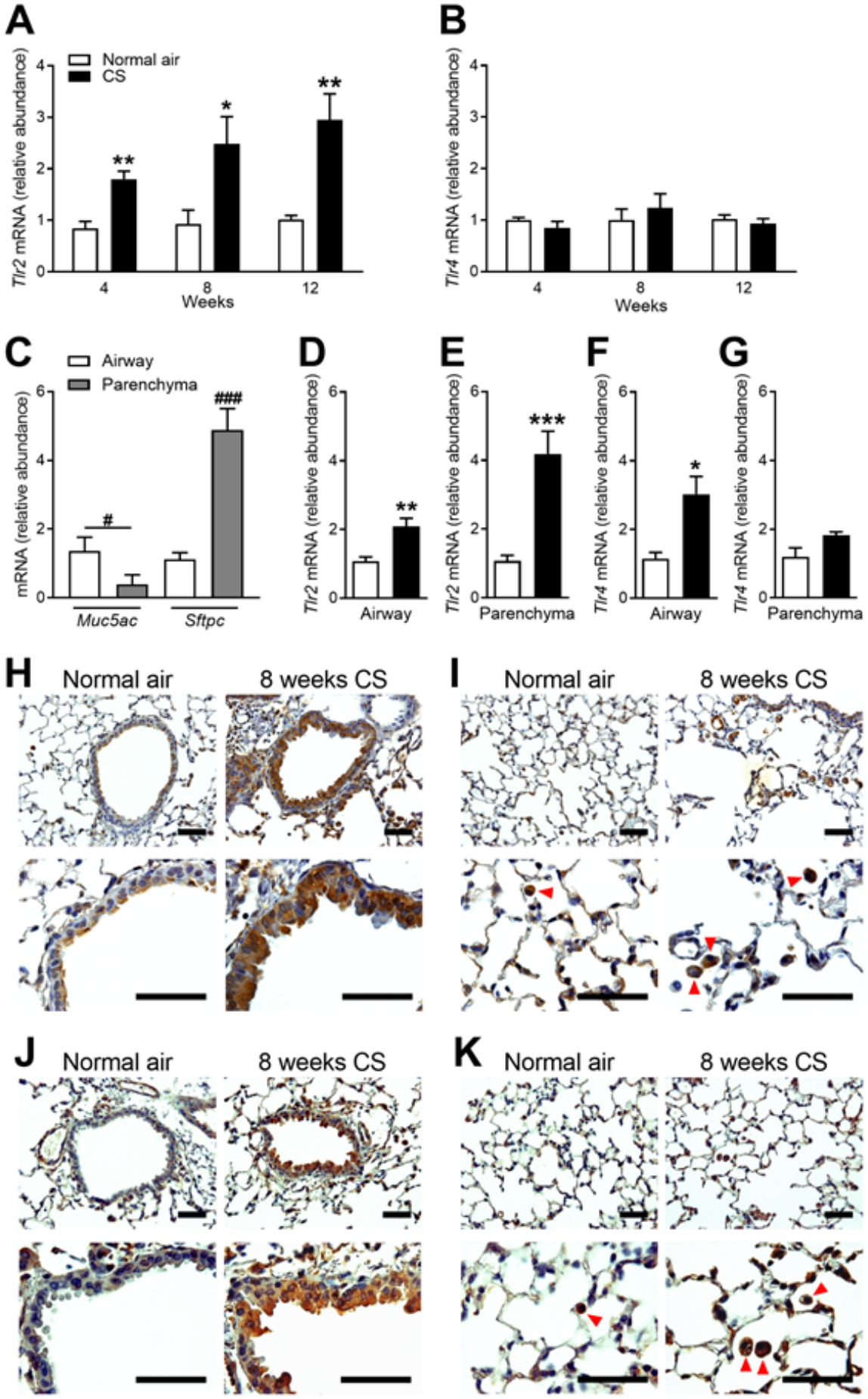
A
Normal air
CS
Tlr2 mRNA (relative abundance)
Weeks
B
Tlr4 mRNA (relative abundance)
Weeks
C
Airway
Parenchyma
mRNA (relative abundance)
Muc5ac
Sftpc
D
Tlr2 mRNA (relative abundance)
Airway
E
Tlr2 mRNA (relative abundance)
Parenchyma
F
Tlr4 mRNA (relative abundance)
Airway
G
Tlr4 mRNA (relative abundance)
Parenchyma
H
Normal air
8 weeks CS
I
Normal air
8 weeks CS
J
Normal air
8 weeks CS
K
Normal air
8 weeks CS

Figure 2

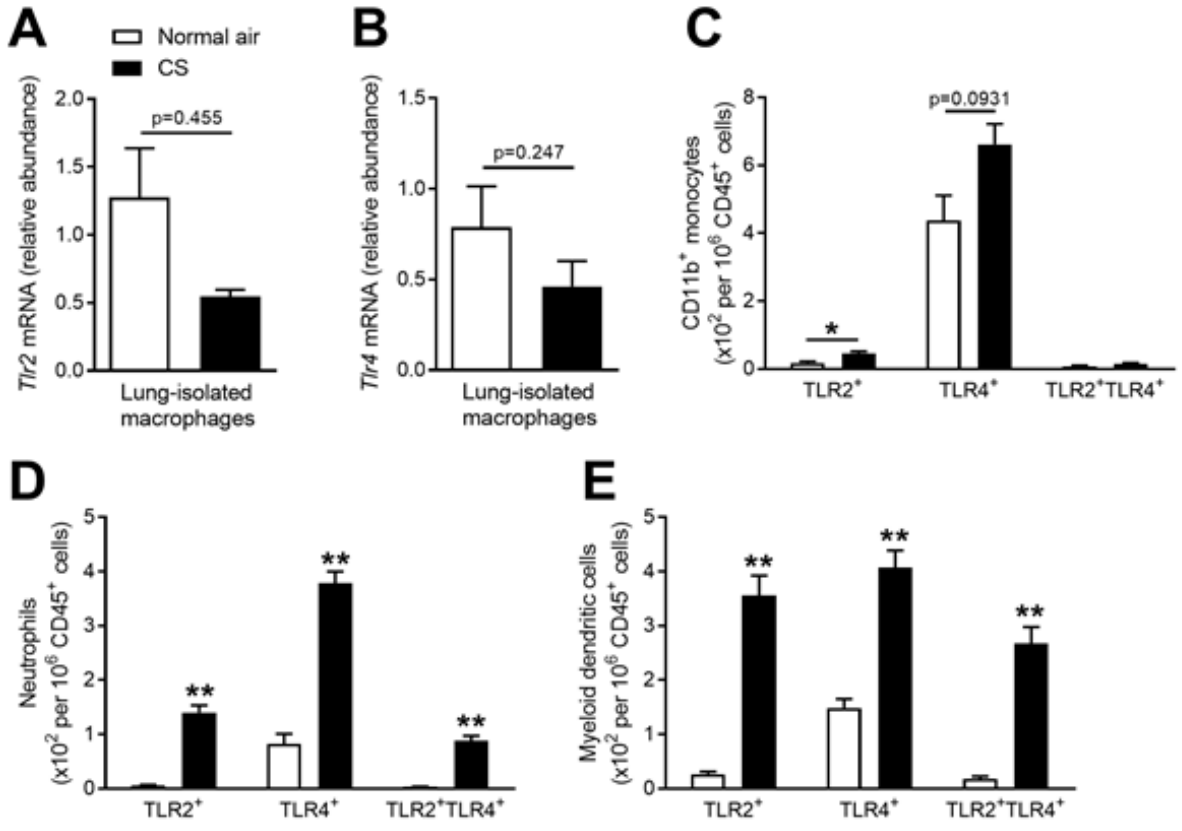
A
Normal air
CS
Tlr2 mRNA (relative abundance)
p=0.455
Lung-isolated macrophages
B
Tlr4 mRNA (relative abundance)
p=0.247
Lung-isolated macrophages
C
CD11b+ monocytes (x10^2 per 10^6 CD45+ cells)
p=0.0931
*
TLR2+
TLR4+
TLR2+TLR4+
D
Neutrophils (x10^2 per 10^6 CD45+ cells)
**
TLR2+
TLR4+
TLR2+TLR4+
E
Myeloid dendritic cells (x10^2 per 10^6 CD45+ cells)
**
TLR2+
TLR4+
TLR2+TLR4+

Figure 3

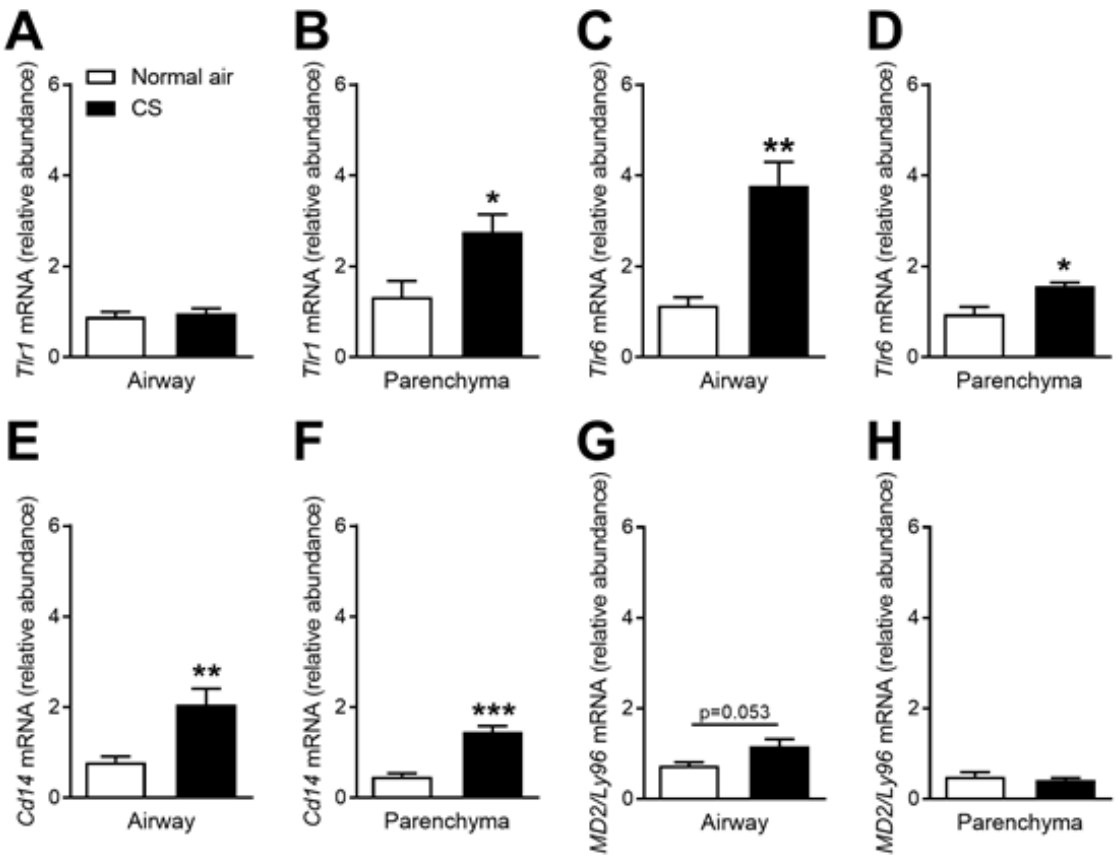
A
B
C
D
E
F
G
H
Normal air
CS
Tlr1 mRNA (relative abundance)
Tlr6 mRNA (relative abundance)
Cd14 mRNA (relative abundance)
MD2/Ly96 mRNA (relative abundance)
Airway
Parenchyma
*
**
***
p=0.053
0
2
4
6

Figure 4

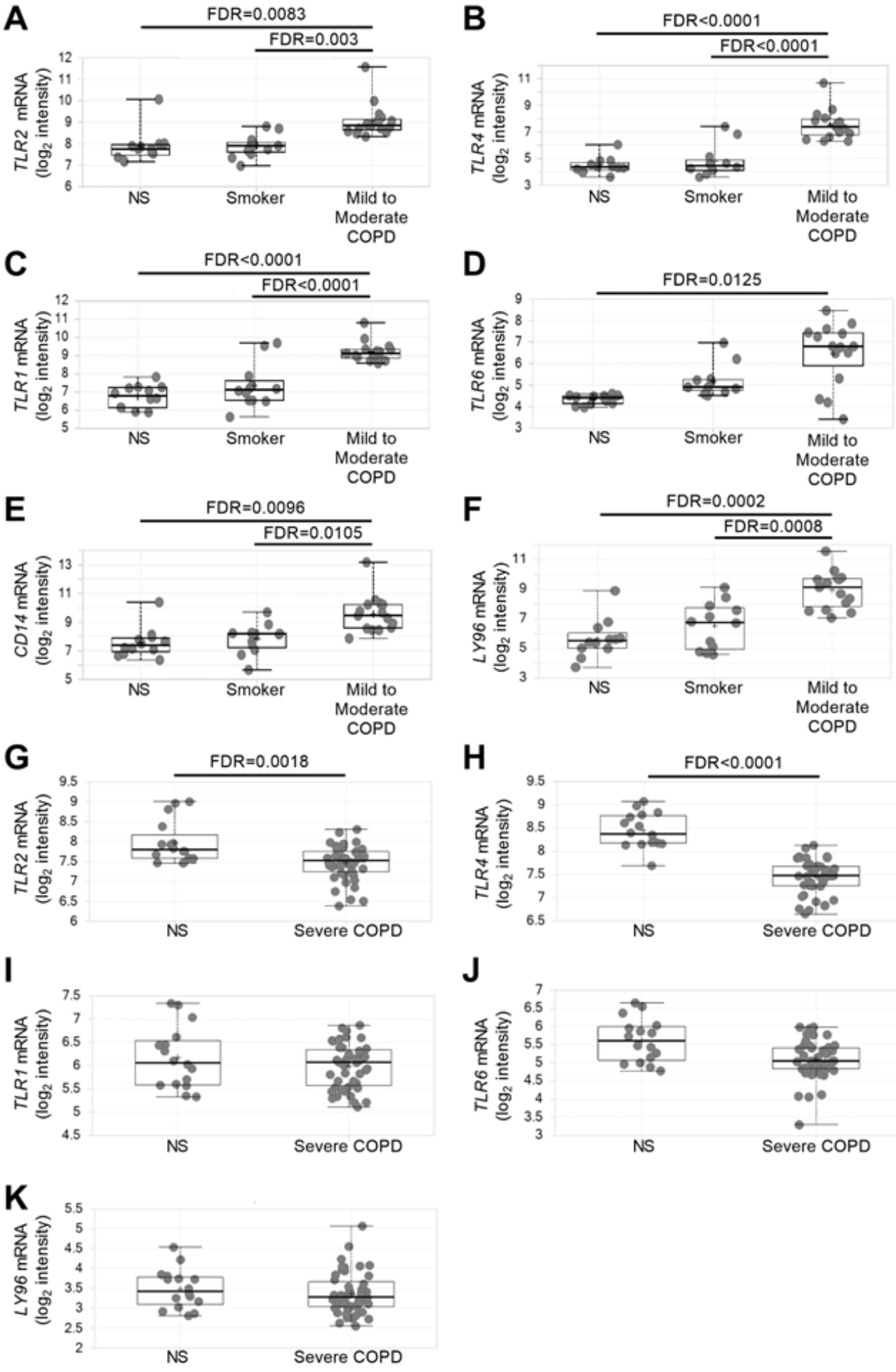
A
FDR=0.0083
FDR=0.003
TLR2 mRNA (log2 intensity)
NS
Smoker
Mild to Moderate COPD
B
FDR<0.0001
FDR<0.0001
TLR4 mRNA (log2 intensity)
C
FDR<0.0001
FDR<0.0001
TLR1 mRNA (log2 intensity)
D
FDR=0.0125
TLR6 mRNA (log2 intensity)
E
FDR=0.0096
FDR=0.0105
CD14 mRNA (log2 intensity)
F
FDR=0.0002
FDR=0.0008
LY96 mRNA (log2 intensity)
G
FDR=0.0018
TLR2 mRNA (log2 intensity)
NS
Severe COPD
H
FDR<0.0001
TLR4 mRNA (log2 intensity)
I
TLR1 mRNA (log2 intensity)
J
TLR6 mRNA (log2 intensity)
K
LY96 mRNA (log2 intensity)

Figure 5

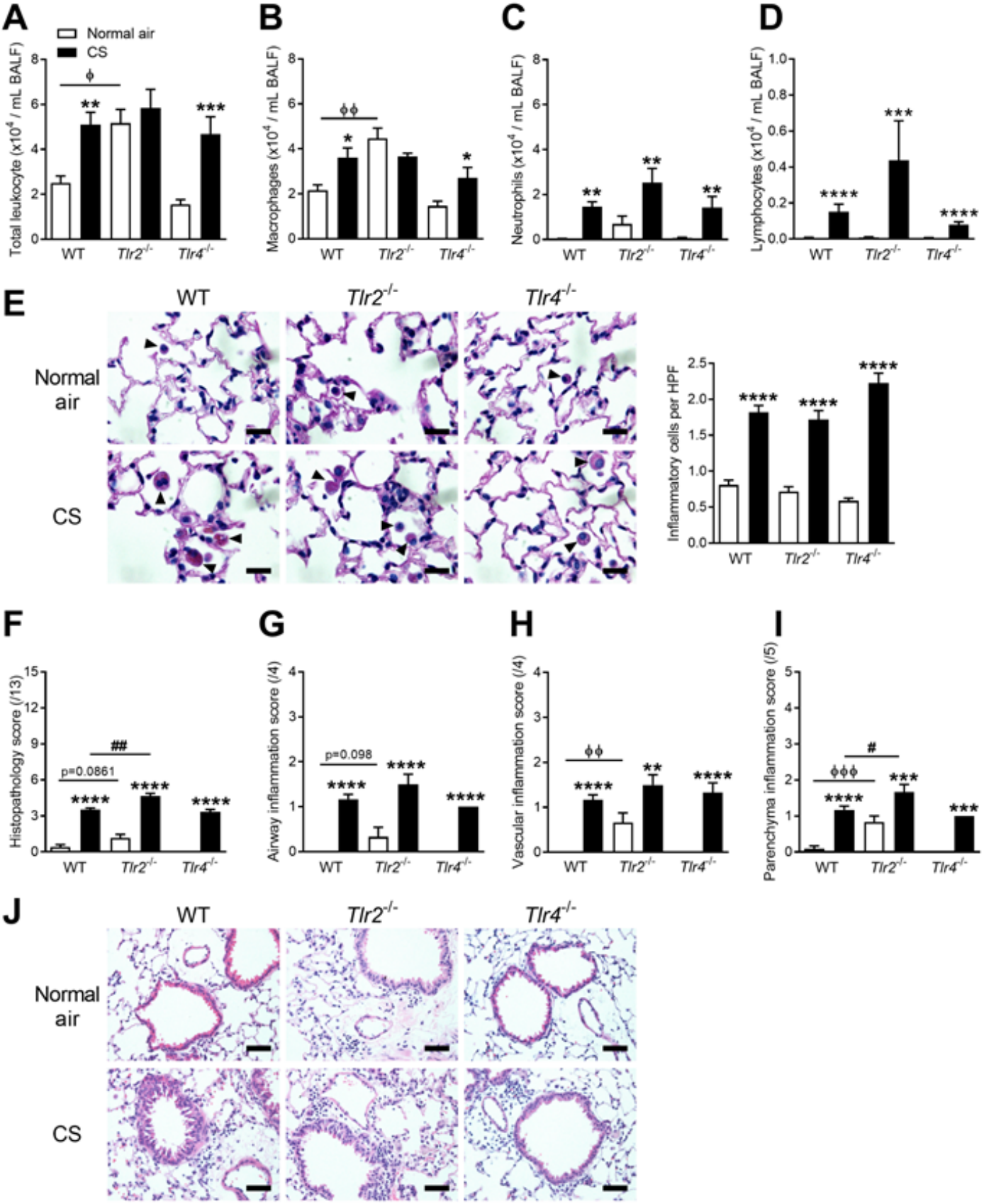
A
Normal air
CS
Total leukocyte (x10⁴ / mL BALF)
B
Macrophages (x10⁴ / mL BALF)
C
Neutrophils (x10⁴ / mL BALF)
D
Lymphocytes (x10⁴ / mL BALF)
WT
Tlr2-/-
Tlr4-/-
E
Normal air
CS
Inflammatory cells per HPF
F
Histopathology score (/13)
p=0.0861
G
Airway inflammation score (/4)
p=0.098
H
Vascular inflammation score (/4)
I
Parenchyma inflammation score (/5)
J

Figure 6

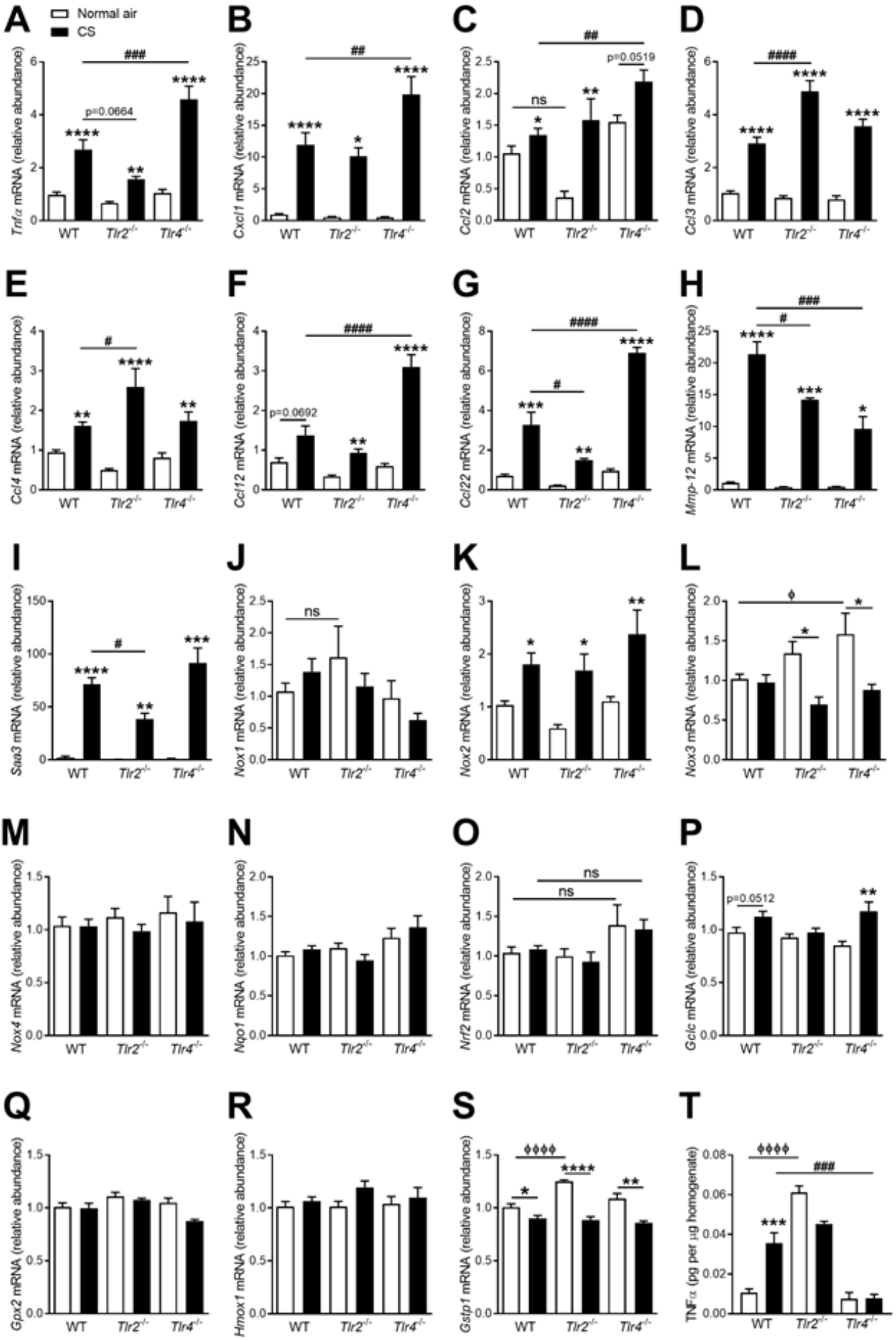
A
Normal air
CS
Tnfα mRNA (relative abundance)
p=0.0664
###
****
**
****
B
Cxcl1 mRNA (relative abundance)
##
****
*
****
C
Ccl2 mRNA (relative abundance)
##
ns
*
**
p=0.0519
D
Ccl3 mRNA (relative abundance)
####
****
****
****
E
Ccl4 mRNA (relative abundance)
#
**
****
**
F
Ccl12 mRNA (relative abundance)
####
p=0.0692
**
****
G
Ccl22 mRNA (relative abundance)
####
#
***
**
****
H
Mmp-12 mRNA (relative abundance)
###
#
****
***
*
I
Saa3 mRNA (relative abundance)
#
****
**
***
J
Nox1 mRNA (relative abundance)
ns
K
Nox2 mRNA (relative abundance)
*
*
**
L
Nox3 mRNA (relative abundance)
ϕ
*
*
M
Nox4 mRNA (relative abundance)
N
Nqo1 mRNA (relative abundance)
O
Nrf2 mRNA (relative abundance)
ns
ns
P
Gclc mRNA (relative abundance)
p=0.0512
**
Q
Gpx2 mRNA (relative abundance)
R
Hmox1 mRNA (relative abundance)
S
Gstp1 mRNA (relative abundance)
ϕϕϕϕ
*
****
**
T
TNFα (pg per μg homogenate)
ϕϕϕϕ
###
***
WT
Tlr2-/-
Tlr4-/-

Figure 7

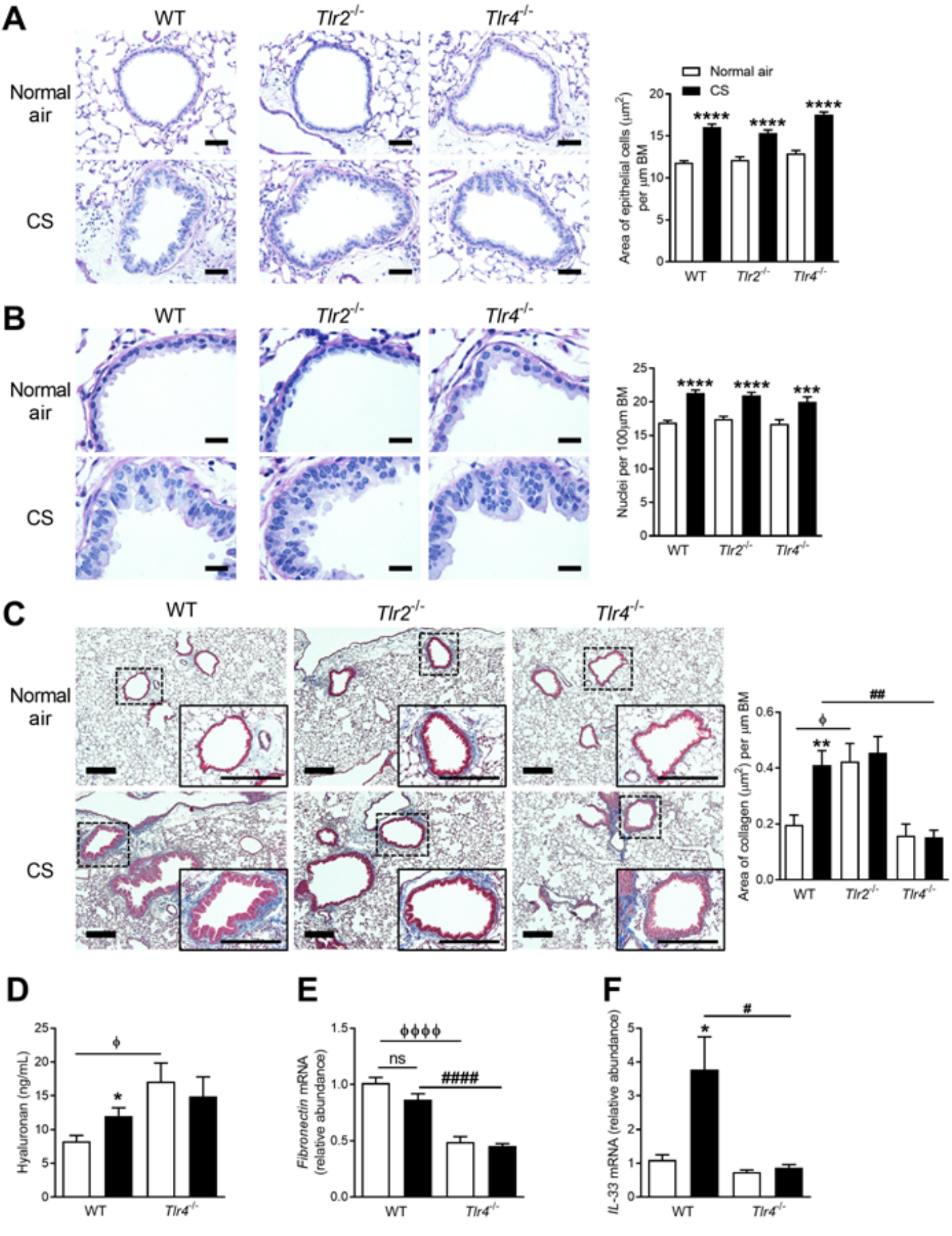
A
WT
Tlr2-/-
Tlr4-/-
Normal air
CS
Normal air
CS
Area of epithelial cells (µm2) per µm BM
****
****
****
WT
Tlr2-/-
Tlr4-/-
B
WT
Tlr2-/-
Tlr4-/-
Normal air
CS
Nuclei per 100µm BM
****
****
***
WT
Tlr2-/-
Tlr4-/-
C
WT
Tlr2-/-
Tlr4-/-
Normal air
CS
Area of collagen (µm2) per µm BM
ϕ
**
##
WT
Tlr2-/-
Tlr4-/-
D
Hyaluronan (ng/mL)
ϕ
*
WT
Tlr4-/-
E
Fibronectin mRNA (relative abundance)
ϕϕϕϕ
ns
####
WT
Tlr4-/-
F
IL-33 mRNA (relative abundance)
#
*
WT
Tlr4-/-

Figure 8

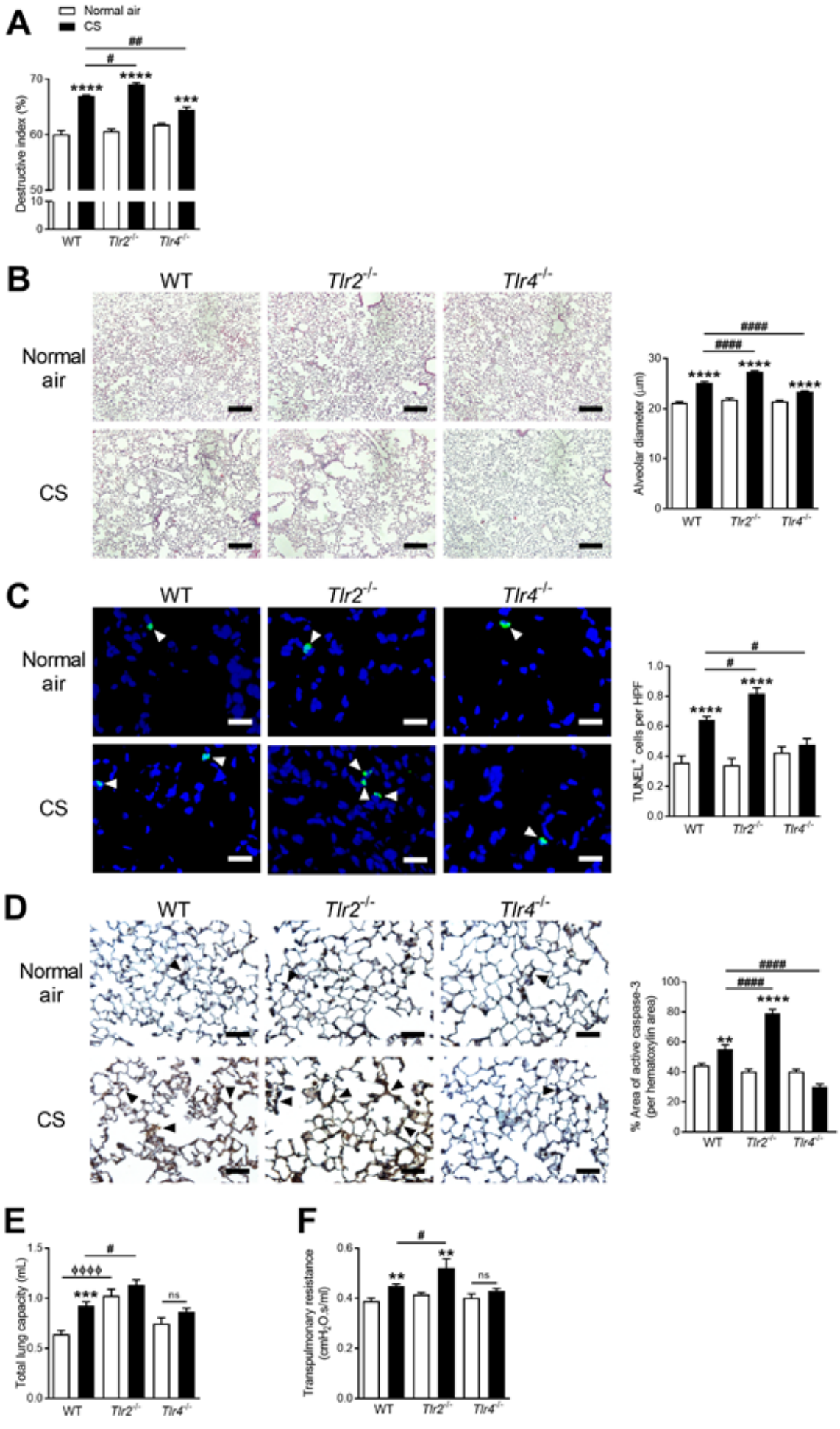
A
Normal air
CS
Destructive index (%)
WT
Tlr2-/-
Tlr4-/-
B
WT
Tlr2-/-
Tlr4-/-
Normal air
CS
Alveolar diameter (µm)
C
TUNEL+ cells per HPF
D
% Area of active caspase-3 (per hematoxylin area)
E
Total lung capacity (mL)
F
Transpulmonary resistance (cmH2O.s/ml)